Report 74-14 July 1974

USE OF THE ARMORED T-28 AIRCRAFT TO OBTAIN OBSERVATIONS IN HAILSTORMS WITH EMPHASIS ON THE CHARACTERISTICS OF THE HIGH RADAR REFLECTIVITY ZONES

By: Wayne R. Sand

Prepared for:

National Science Foundation
Washington, D. C. 20550

NSF Grant GA 182-71

Institute of Atmospheric Sciences

South Dakota School of Mines and Technology

Rapid City, South Dakota 57701

FOREWORD

This report was prepared by Mr. Sand in 1974 as a Master's thesis in the Department of Meteorology of the South Dakota School of Mines and Technology. Professor Dennis J. Musil served as Mr. Sand's thesis advisor.

ABSTRACT

This study relates data gathered during the penetration of hailstorms between 4.9 and 6.7 km MSL (16,000 and 22,000 ft) by an armored T-28 aircraft to detailed radar data of the hailstorms penetrated. These data recorded by the T-28 data system are combined with observations made by the author while piloting the T-28 through hailstorms. The radar data from the National Hail Research Experiment CPR-2 are specially prepared as Constant Altitude Plan Position Indicator (CAPPI) displays and vertical sections along the aircraft track for comparison with the data gathered by the aircraft system and pilot's observations.

The T-28 penetration vehicle is described in detail. All pertinent data acquisition techniques along with data limitations are discussed in detail.

The results indicate that significant updrafts are frequently found well ahead of the high radar reflectivity zones. The updrafts are found to be relatively smooth while the high radar reflectivity zones are found to be very turbulent. Significant quantities of supercooled liquid water are found in the inflow regions. The most significant airframe icing is found in the strong updrafts while the high reflectivity zones are found to contain almost exclusively ice. Hail is most frequently found in the area of strong reflectivity gradient but small hail is found outside the 40 dBz contour.

LIST OF FIGURES

1. INTRODUCTION

A modified North American T-28 (Fig. 1) aircraft was flown through thunderstorms by the author as part of the National Hail Research Experiment (NHRE) during the 1972 field season. There were 83 thunderstorm penetrations made, many of which encountered hail. Hail, turbulence, lightning and icing observations were voice recorded during the penetrations. Time, altitude, updrafts, turbulence and Johnson-Williams liquid water content (JW LWC) data were collected by the onboard data system. A radar system located at Grover, Colorado (Fig. 2) took detailed quantitative radar measurements during these penetrations. The radar data were computer processed to generate vertical sections of radar reflectivity factor along the aircraft track and Constant Altitude Plan Position Indicator (CAPPI) displays each kilometer of elevation above sea level. The study was focused on observations from three days (21 June, 7 July and 22 July 1972), consisting of seven storm penetrations. Data from all sources were of high quality on these three days.

The three data sources (radar, aircraft and personal observations) will be discussed in detail. The data recorded on the aircraft meteorological data system and the pilot's observations are used to describe the composition of the hailstorms with emphasis on the characteristics of the high radar reflectivity zones.

The relationship of the high reflectivity zone to the following will be discussed in detail: 1) updrafts, 2) liquid water content, 3) turbulence, 4) hail, 5) icing, and 6) lightning.

Fig. 1. T-28 armored aircraft used for hailstorm penetrations.

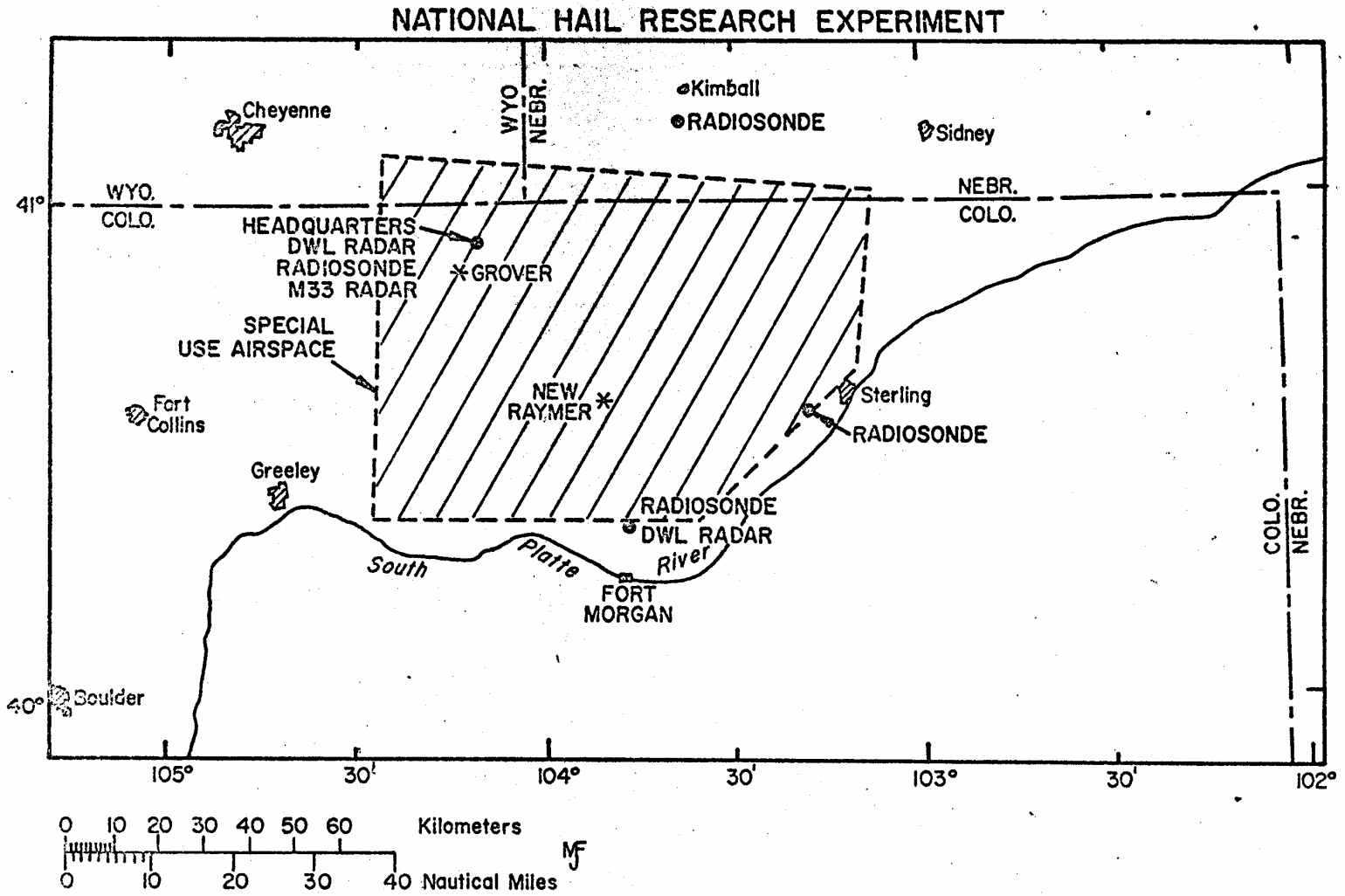

Fig. 2. NHRE Opefations Area.

2. BACKGROUND AND OBJECTIVES

The Thunderstorm Project (Byers and Braham, 1949) made first mention of using an aircraft to penetrate thunderstorms to acquire scientific data in the region of high reflectivity. Direct measurement of the interior of hailstorms became more intriguing over the years until in 1968 work started on the development of a special aircraft for this task, one that could withstand hail encounters with minimal danger. The modified, armor plated T-28 aircraft first flew into thunderstorms in 1970 as part of the Northeast Colorado Hail Experiment. Following this first encouraging season the aircraft was plagued with engine problems, forcing it to miss the 1971 season. The armored T-28 was contracted to the NHRE in 1972 to act as a thunderstorm penetration vehicle for the purpose of gathering data in a region heretofore inaccessible to research meteorologists.

The overall objective of the research is to use the armored T-28 to obtain data within and in the immediate vicinity of hailstorms (Sand et al., 1972b). The specific objectives are:

1. Obtaining measurements of updrafts in regions of hail formation and growth;
2. Determining the composition of high radar reflectivity zones; and
3. Studying ice-water budgets in hailstorms.

The objectives of the NHRE project (Swinbank, 1970) are:

1. Gain an increased understanding of all aspects of the cloud dynamics and microphysics governing the severe convective storms that produce damaging hailfall at the ground; and

2. Equipped with this increased knowledge to develop, if possible, a method for suppressing the occurrence of damaging hail.

The first objective of the NHRE project and the second objective of the T-28 project are treated in this study.

3. PENETRATION VEHICLE

A North American T-28A has been modified and armor plated to be used as a thunderstorm penetration vehicle. The T-28 has a gross weight of 4,086 kg (9,000 lbs) and is capable of performing at altitudes in excess of 7.62 km (25,000 ft.) since its original 700 horsepower engine has been replaced with a 1425 horsepower engine. The highly modified and armor plated T-28 seen in Fig. 1 is by no means standard. The figure does not show many of the subtle changes in the aircraft to make it suitable for the job of penetrating hail bearing thunderstorms in turbulent and icing conditions.

The armor plating on the T-28 added about 318 kg (700 lbs) mass to the aircraft and covered all the leading edges with extra metal. The leading edges of the wing and tail surfaces were covered with 2.29 mm (0.090 in) 2024T4 aluminum sheets formed to fit and bonded to the existing wing and tail surfaces (Fig. 3). The tops of the wings were covered with 0.81 mm (0.032 in) sheets of the same material. The leading edges of the cowling were covered with an additional sheet of fitted 3.18 mm (0.125 in) aluminum. The carburetor was protected from ingestion of large hailstones by the addition of a metal grate to break up the hailstones prior to entry. A similar device was installed over the oil cooler intake to prevent damage to the relatively fragile oil radiator.

The canopy required substantial modification since the standard plexiglass canopy was much too weak to withstand encounters with large hail. The windshield was replaced with flat sheets of 1.91 cm (0.75 in) stretched acrylic and the side panels were made of flat sections of 1.52 cm (0.60 in) stretched acrylic (Fig. 4). The windshield and armor

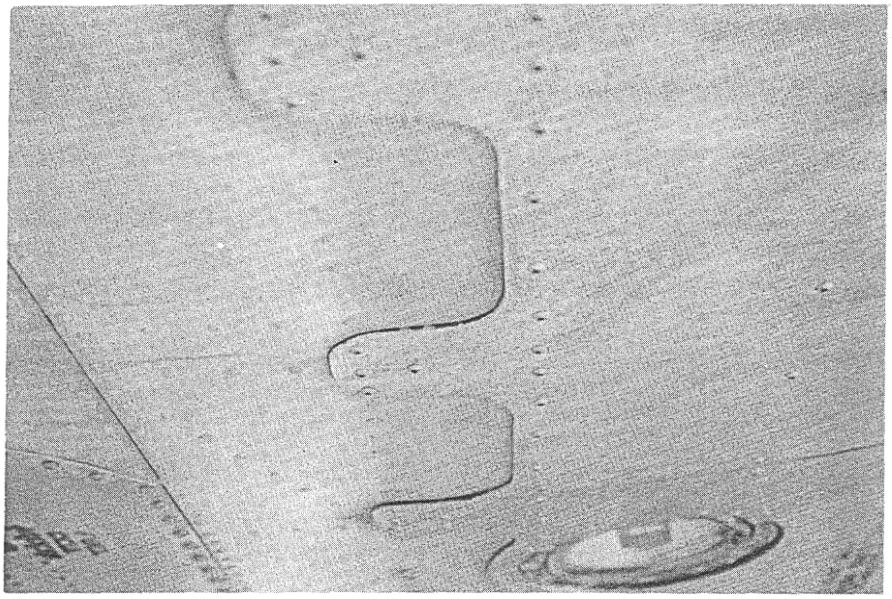

Fig. 3. Armor plating on T-28 wings. Note 2.29 mm (0.090 in) armor on leading edges.

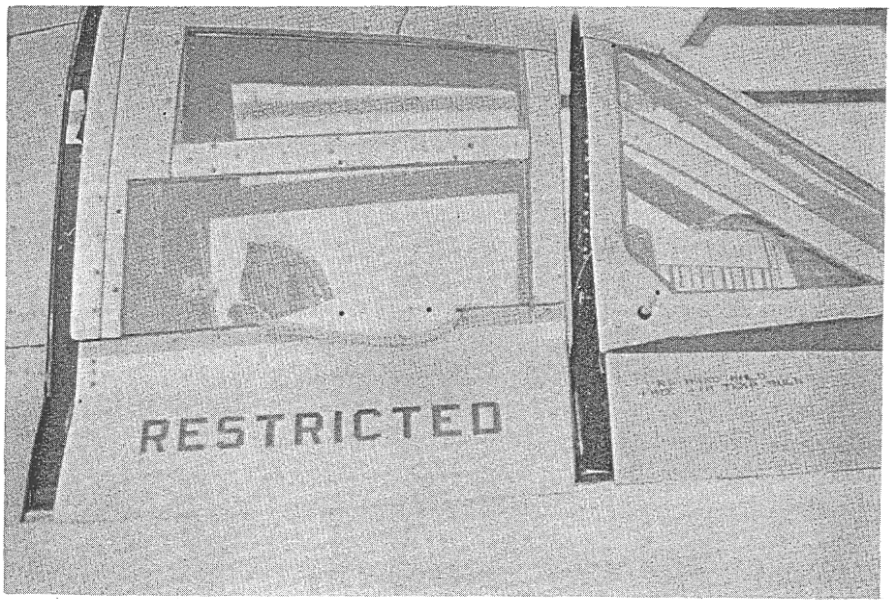

Fig. 4. Armor plating on T-28 canopy. Note heavy metal and stretched acrylic structure.

plating were tested to withstand impacts from 7.62 cm (3.0 in) hail at 100 m sec^{-1} (200 kts) with minimal damage (Williamson, 1969).

A new engine installed in 1972 required a different scheme for protecting it from hail damage since it is a slightly different model than the engine originally armored and tested for hail damage. The result can be seen in Fig. 5. Note that the push rod housings and the ignition harness are protected with sections of electrical conduit pipe formed to fit the respective areas. The propeller governor is protected with a piece of angle iron.

The T-28 is equipped with alcohol deicing for the propeller and the carburetor. If these two areas can be kept clear of ice the engine will continue to develop full power. The T-28 is able to carry a substantial load of ice on the airframe since it is considerably overpowered.

Since a distinct possibility exists that the entire electrical system could be disabled by a lightning strike or an overload on the system, proper precautions were necessary to enable continued safe flight with the T-28 in the event of electrical problems. The aircraft has a 300 ampere generator which is being used to the maximum authorized output during a penetration when all the sensing, recording, and deicing equipment is operating. To protect against possible equipment failures there are not only double circuit breakers on all the high power equipment but switches which are easily accessible to the pilot so he may turn off any or all scientific equipment in the event of an electrical problem. A primary flight attitude panel (consisting of a needle, ball and airspeed) was not considered adequate for continued safe flight in the severe environment of a thunderstorm. Therefore, the T-28 has been equipped with dual artificial horizons, one electrical and the other

vacuum driven to enable continued safe flight in the event of complete electrical failure. The breathing oxygen system provides safe reliable operation to well over 10.69 km (35,000 ft). The pilot always carries a current parachute. Military experience with the T-28 indicates a high probability of a safe bailout in the event of an emergency.

Wherever possible the instrumentation is integrated into the airplane and pods are not carried. An example of this is the right wingtip (Fig. 6) where four instruments are carried mounted within and on the wingtip and directly to the skin of the aircraft wing.

A more complete description of the aircraft and the data system may be found in Sand et al. (1972b), Sand et al. (1973) and Johnson (1974).

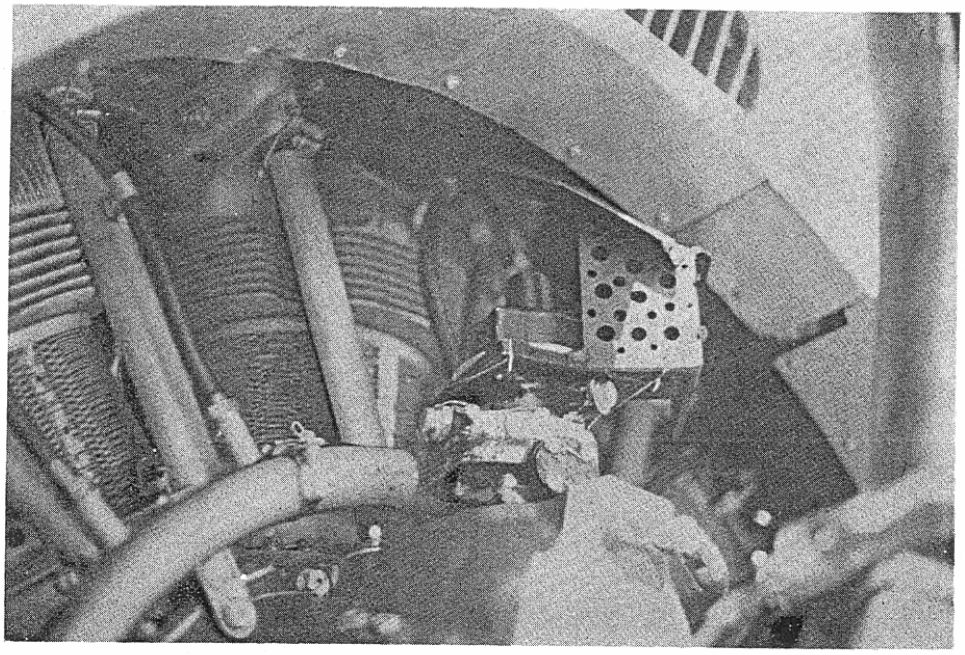

Fig. 5. Armor plating on T-28 engine. Note armored ignition harness, push rod housings and propeller governor.

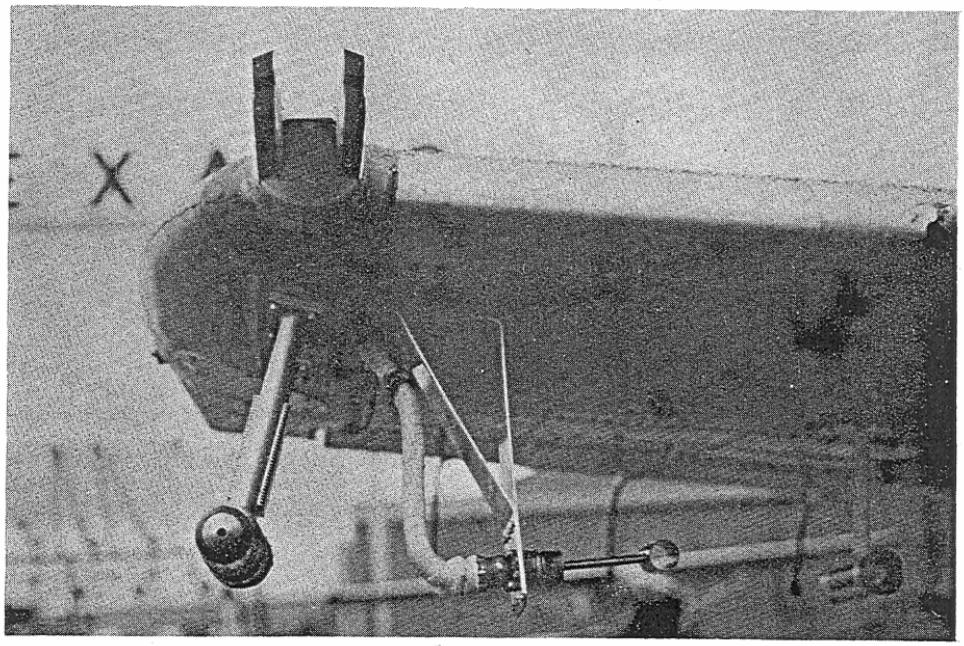

Fig. 6. Four instruments mounted on T-28 right wing tip.

4. HAILSTORM PENETRATION TECHNIQUE

Considerable effort has been devoted to the development of a hailstorm penetration technique to insure flight safety and to maximize data collection. The basic procedure is that a highly qualified meteorologist with access to a radar system is in charge of vectoring the aircraft into desired areas of a storm. The vector selected normally permits penetration of a maximum radar reflectivity zone as well as an updraft at aircraft altitude.

A limit has been imposed on the maximum radar reflectivity permitted for penetration. This reflectivity limit was set based on reports by Chisholm (1968) and Dennis et al. (1971). The limit is 55 dBz at the altitude of penetration. This criterion was selected to permit the aircraft to encounter hail, but to avoid hail of a destructively large size. The maximum hail encountered using this limit has been 1.9 cm (0.75 in) diameter as estimated by the pilot.

A normal flight consists of from three to six penetrations and is limited by the one hour of data tape carried on the aircraft and the limited fuel supply (2.5 hours). Normally, one hour of data tape is sufficient because the tape recorder operates only during penetrations.

Typical operational procedure is to begin penetrations at 7.32 or 6.70 km MSL (24,000 or 22,000 ft MSL) and proceed downward at 0.61 km (2,000 ft) intervals on successive penetrations until 4.88 km (16,000 ft) is reached (Fig. 7). This routine is interrupted on occasions when airframe ice builds up to a point where the pilot considers another penetration unwise. Further penetrations are then merely delayed until a descent is made to melt the accumulated ice.

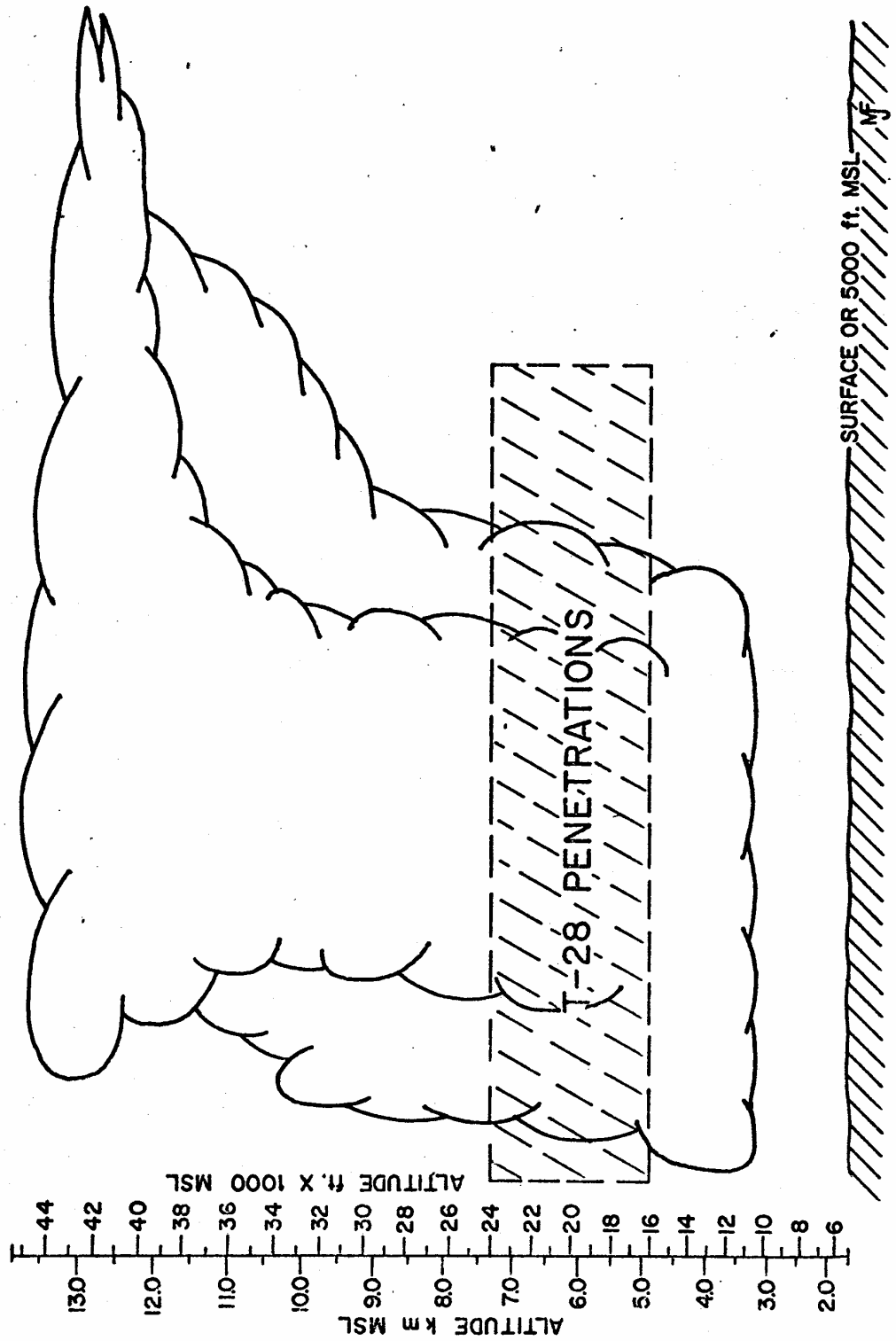

Fig. 7. T-28 hailstorm penetration profile.

The research flight paths are controlled by the Denver Air Route Traffic Control Center and the T-28 is given a ±1.22 km (±4,000 ft) altitude clearance to compensate for the frequently strong up- and downdrafts encountered. The +1.22 km (+4,000 ft) clearance limit is reached occasionally, but rarely exceeded.

Once the T-28 was launched, based on the existence of a suitable thunderstorm in the NHRE operating area, the ground based meteorologist selected an area of the storm for penetration based on real-time radar data. The T-28 was then vectored to an initial point so that a penetration could be made along a track that would encounter a high reflectivity zone and an updraft. The pilot would then turn on all the necessary equipment and set up for cloud penetration by stabilizing the aircraft at a cruise power setting and airspeed. Once the penetration began, an attempt was made to maintain an attitude and airspeed with no power changes (altitude is allowed to fluctuate). However, power changes occurred if the altitude fluctuated and airspeed changed as a result of turbulence and updrafts.

When a cloud penetration begins the recorders are in the "continuous" mode and all microphones are "hot" so the pilot can record a running commentary of his observations. Timely information on radar reflectivities and storm progress is received from the radar site and recorded as is the sound of any hail encountered.

Penetrations are normally made with a constant heading until clear air is encountered or until the T-28 is well clear of any radar echoes. The aircraft then reverses course and changes altitude in preparation for another penetration.

The problem of greatest concern during penetrations is the occasional

occurrence of extremely rapid ice accumulation (often at an observed rate of 2.5 cm (1.0 in) per minute). This has the effect of very rapidly increasing the weight and changing the aerodynamics of the T-28. When the air intake to the carburetor and oil cooler is constricted by ice accumulation in such icing situations, a loss of power and high oil temperature results. Limited airflow to the carburetor can be regained with the addition of carburetor heat. This procedure uses air from inside the cowling resulting in a loss of power. The oil cooler also has a special alternate air source from inside the cowling. The carburetor and oil cooler intakes are protected from large hail ingestion by the grates described earlier and these grates provide the surface areas for heavy ice accumulation in high supercooled liquid water content regions of the cloud. Induction system icing has not caused a complete engine failure but has caused some moments of concern for the pilot.

Because of the adverse conditions in which the aircraft operates and the comparatively abusive treatment that it gets, high quality maintenance is imperative. This is provided for by the employment of a mechanic whose chief responsibility is the meticulous care of the T-28. Normal maintenance includes a very detailed inspection before and after each research flight by both the pilot and the mechanic. The engine is checked at regular intervals to detect any possible damage from rapid heating and cooling during penetrations. An oil sample is subjected to spectrometric analysis for metals at regular intervals to check for any abnormal internal wear. Only knowledgeable and qualified personnel are allowed to work around the aircraft and all work is checked and double checked. All modifications on this restricted category aircraft are approved by the Federal Aviation Agency.

5. DATA SOURCES

The data gathered falls into three catagories; data from aircraft instrumentation system, pilot's observations and ground based radar data. The source, acquisition and relative accuracy of all data used is discussed in detail in the following sections.

5.1 Data from Aircraft Instrumentation System

The data gathered with the T-28 system consisted of 17 channels of analog data, (Table 1) recorded every 0.67 seconds by a Metrodata DL-620 magnetic tape recorder.

Only seven of the recorded parameters are used in this analysis. They are: time, rate-of-climb, pressure, Johnson-Williams liquid water content (JW LWC), indicated airspeed, manifold pressure and temperature. These variables are further reduced to the five variables of interest (time, updrafts, altitude, JW LWC and turbulence) and only these are discussed in detail.

5.1.1 Time

At the outset of the 1972 field season the recording of time was felt to be a rather routine exercise requiring minimal attention. As it turned out the discrepancies in time between the T-28, the CPR-2 data acquisition radar and the M-33 tracking radar presented significant data reduction problems.

Time in the T-28 is generated in the DL-620 data recorder by a crystal controlled oscillator and synchronized prior to each flight with the clock used to set the time in the CPR-2 and the M-33 radars which in turn is set daily with the WWV standard time. Normally this procedure should provide adequate time correlation but this was not always the case.

TABLE 1

T-28 Data Recorded

Channel	Parameter	Used in this study	Units
1, 2	Time	*	hr min sec
3	Ball Pressure	*	Altitude ft MSL
4	Indicated Airspeed	*	Kts
5	VOR		
6	WSI Pressure		
7	DME		
8	Manifold Pressure	*	In Hg
9	Rosemount Temperature		
10	WSI Temperature	*	C
11	J. W. Liquid Water Content	*	$g\ m^{-3}$
12	Rate-of-climb	*	$m\ sec^{-1}$
13	Regulated 5 Volts		
14	Accelerometer		
15, 16	Kyle Evaporator		
17	Spare		
18	Spare		
19	Event Code	*	In cloud/Out cloud
20	Spare		

The comments recorded during the cloud penetrations were referenced to a direct readout of DL-620 time so pilot's comments and aircraft data are exactly related in time. The CPR-2 radar system time, recorded with the radar data, had no capability for direct readout so that errors introduced by frequent power outages of the rural power source remained undetected during the data logging sequence. The M-33 track radar times were manually recorded by the operator directly onto the trace of aircraft track generated by the M-33 plotting system.

Since all data is very critically related to time, these various sources of time errors generated problems. Where time discrepancies existed between the M-33 track radar and the aircraft systems, the times were synchronized by using the pilot's voice recording, noting the time of heading changes to synchronize these data. Therefore, the aircraft data and the pilot's comments are felt to be within a few seconds of the track data in all cases.

The errors in the CPR-2 radar data were usually accurately corrected during computer analysis. The computer analysis of the CPR-2 radar data can also introduce time errors during the generation of vertical sections and CAPPI displays which appear to exceed the minor errors in the raw data. These CPR-2 data space-time errors are discussed in section 5.3.2. The reflectivity data are not felt to differ from the aircraft data by more than about two minutes due to this space-time problem and the clock errors in the data.

5.1.2 Updrafts

The relative accuracy and rapid response of an aircraft to an updraft is due to the manner in which the aircraft responds to vertical motions. If the aircraft responded to the current of air because of its

surface area normal to the flow, the response would be slow indeed. The aircraft responds to the vertical component of air velocity due to a change in angle-of-attack of the airfoils causing a change in the total lift which can translate to either an increase in airspeed or rate-of-climb. Since the aircraft is inherently stable in terms of airspeed it will tend to respond to these angle-of-attack changes by increasing or decreasing its rate-of-climb very rapidly.

The updrafts as given in lower part of Figs. 8A-G are a refinement of the rate-of-climb values measured by the aircraft. The refinement of the rate-of-climb values is an improvement of the system used by Auer and Sand (1966) and Auer and Marwitz (1973). The present values of rate-of-climb are recorded from a Ball model 101A variometer. The rate-of-climb values are corrected for deviations in airspeed and manifold pressure by the following equation:

$$U = ROC + ((27-MAP)\ 92.0 + (IAS - 140)\ 17.7)\ 0.00508 \qquad (1)$$

U = updraft in m sec^{-1}

ROC = rate-of-climb in m sec^{-1}

MAP = manifold pressure in inches of mercury

IAS = indicated airspeed in knots

Equation 1 was empirically determined from data obtained during a test flight for that purpose on 28 July 1972. The updraft data are felt to be within 2 m sec^{-1}.

The manifold pressure fluctuations are caused by changes in altitude since the engine will lose approximately one inch of mercury manifold pressure for each 305 m (1,000 ft) of altitude gained in an updraft if the throttle setting is left unaltered. The manifold pressure also fluctuates as a result of icing in the induction system and over

the carburetor intake protection grate.

The airspeed will fluctuate as a result of turbulence, updrafts and due to pilot induced attitude changes when entering and exiting updrafts. That is, the normal pilot reaction is to put the nose down slightly, thus increasing airspeed when entering a strong updraft. The opposite reaction is normal when exiting the updraft or entering a downdraft i.e., the pilot will tend to pull the nose up slightly thus decreasing the airspeed.

The T-28 system is easily capable of responding to an updraft with a 500 meter (1,640 ft) diameter since that represents approximately 5 sec flight time. The limiting response time is felt to be nearer to 2 or 3 sec.

It should be emphasized that no attempt was made to measure the rapid short term gusts described by Sinclair (1969) because these measurements require a gust vane system and none of the systems currently available are capable of withstanding the hail and icing environment in which the T-28 flies.

5.1.3 Altitude

The altitude traces on the lower part of Figs. 8A-G are derived from measurements of pressure made with a Ball model EX-210-B pressure transducer. The pressure transducer is assumed linear in the range from 4.57 to 7.62 km MSL (15,000 to 25,000 ft) which introduces an error of not more than 45 m (148 ft). Since the instrument is not perfectly linear in this range and it is not temperature compensated, the error is reasonable. The pressure transducer was calibrated using an accurate pressure reference standard manometer at the University of Wyoming aviation facility on 22 June 1972.

The altitude fluctuations during penetrations discussed herein were well within the 4 to 7 km MSL (13,000 to 23,000 ft), used in Figs. 8A-C.

5.1.4 Johnson-Williams Liquid Water Content

The JW LWC meter is designed around the principle of changing the resistance in a hot wire due to cooling resulting from small droplets of liquid water striking the wire. The unit is compensated for airspeed and has a meter in the cockpit visible to the pilot for use during in-flight calibration.

The JW LWC device measures liquid cloud droplets with diameter less than 50 um (Ruskin, 1967) so is of little use in measuring total water concentration in regions of the thunderstorm where it is felt that the values can reach 15 gm m^{-3}, according to measurements published by Kyle and Sand (1973).

The adiabatic liquid water concentration is about 1.5 to 3.0 gm m^{-3} at penetration altitudes. Since the maximum value of JW LWC measured during these penetrations was 0.93 gm m^{-3}, the device is suspect of measuring values that are too low. The indication is that either the instrument is giving values that are too low, or the water is in the form of ice, or the liquid water present is in droplets larger than 50 um diameter. The reason for the low reading on the JW LWC device could be any or all of the above, but in general it is felt that the instrument does a very good job of indicating areas containing super-cooled droplets less than 50 um in diameter. Thus, areas of supercooled cloud liquid water concentration which could be a source of hail growth material are indicated by high readings on the JW LWC device.

5.1.5 Turbulence

Subsequent to the initial data aquisition an objective means was

found to define turbulence in Aerographer's Mate 1 & C (1969), (Navy training manual). This definition is based on the fluctuations in airspeed and is as follows:

Light	:	2.5-7.5 m sec^{-1} (5-15 knots)
Moderate	:	7.5-12.5 m sec^{-1} (15-25 knots)
Severe	:	More than 12.5 m sec^{-1} (25 knots)
Extreme	:	Rapid fluctuations in excess of 12.5 m sec^{-1} (25 knots)

Based on these definitions of turbulence a transparent template was made to permit more objective estimates of turbulence to be made from analog traces of indicated airspeed fluctuations. The template was made so that the airspeed block examined was 20 seconds long, therefore the maximum difference had to be within this 20 second period to qualify for the turbulence classifications as listed above. Indicated airspeed data during each penetration were examined with this device and moderate turbulence or greater was noted on the upper part of Figs. 8A-G.

Since the rapid fluctuations of airspeed in excess of 12.5 m sec^{-1} (25 knots) used as the definition for extreme turbulence were never noted, the only values noted in Figs. 8A-G are moderate and severe, designated by M and S respectively along the top of each figure.

Turbulence can be measured quite accurately using the parameter ϵ, (a dissipation rate of turbulent energy), (MacCready, 1964). This more sophisticated method of measuring turbulence was not used in this study but was found to relate quite well to the pilot's observations (Kyle, 1974) lending even more credence to this simple measure of turbulence.

5.2 Observational data

Observational data is defined as that observed by the pilot during

penetrations and recorded with an onboard stereo voice recorder. The stereo voice recorder was operated continuously during all penetrations. The second channel of the stereo recorder was used to record the sound of hail striking the windshield of the aircraft. Even though the pilot talked to the Grover radar site and the Federal Aviation Agency Air Route Traffic Control Center, he was able to make many observations during thunderstorm penetrations.

5.2.1 Hail Encounters and Hail Size

A hail microphone was mounted behind the windshield and recorded the sound of hail striking the windshield on one channel of the stereo voice recorder. The recorded hail sound was used to define hail encounter duration. Visual observations by the pilot were used as the prime source for information as to the hail size. Hail duration and hail size is included in Table 2 for each penetration and areas of hail encounters are designated on Figs. 8A-G by hatch marks along the aircraft track. These estimates of hail size were made with reference to a commonly used hail sizing system, (Summers and Wojtiw, 1971), i.e. pea, marble, walnut, etc. Due to the substantial aircraft engine noise recorded on the hail microphone channel it is impossible to acquire any more than a subjective estimate of hail concentration during a hailstorm penetration. In a number of cases it was found from the hail microphone data that the pilot did not visually note a hail encounter and size the hail when in fact hail was encountered.

Hail was not defined as such until it reached approximately pea size. The sound of hail striking the windshield is quite distinctive so in all cases of hail encounters, there is no question that hail was encountered and the hail sound duration defines the precise horizontal

extent of the hail.

The sizes of hail were determined in such a subjective manner that there is room to question the actual size of the hail as noted by the pilot, but the sizes are felt to be within the crude sizing criteria listed above. On numerous occasions it was also possible to verify the stone sizes noted in real time by comparing those sizes with dents in various unprotected parts of the airplane after a given flight, lending credence to the sizes noted during the penetrations.

5.2.2 Turbulence

At the time of the penetrations the only turbulence values were those subjectively made by the pilot. These values were based on the following definition of turbulence as listed in Aerographers Mate 1 & C (1969), (Navy training manual).

Light : A turbulent condition during which occupants may be required to use seat belts, but objects in the aircraft remain at rest.

Moderate : A turbulent condition in which occupants require seat belts and occasionally are thrown against the belt. Unsecured objects in the aircraft move about.

Severe : A turbulent condition in which the aircraft momentarily may be out of control. Occupants are thrown violently against the belt and back into the seat. Objects not secured in the aircraft are tossed about.

Extreme : A rarely encountered turbulent condition in which the aircraft is violently tossed about, and is practically impossible to control. May cause structural damage.

The real time estimates of turbulence correlated well with the

more objective method of determining turbulence discussed in Section 5.1.5. In fact the correlation was so consistent that turbulence derived from airspeed fluctuations alone is included in the analysis. The objective method described in Section 5.1.5 gave a continuous turbulence value, whereas the subjective method only gave point values when a voice comment was made relative to the turbulence encountered.

5.2.3 Icing

Appropriate icing rate and ice depth comments are included as part of Figs. 8A-G. All icing data for these figures were taken from the pilot's voice tape since there were no devices on the aircraft to determine quantitatively the icing rate on the airframe.

With the aid of two homemade observational aids developed by the author, it is felt that the estimates of icing depth and rates are quite accurate. One of these devices can be seen in Fig. 10. It is merely an airfoil attached to the side of the canopy within easy view of the pilot with a calibrated probe protruding from the leading edge. The pilot can thus easily read the depth of ice on the small airfoil (using the calibrated scale) at any time during a penetration. By keeping track of the previous depths as part of the voice tape record and taking the difference the ice accumulated during a given penetratio can be determined.

The readings from this device were combined with the readings from a painted strip on the leading edge of the wing that was in the form of a checker board so that the squares could be counted to determine how far the ice had progressed from the leading edge aft on the upper surface of the wing.

These two visual aids and the rate at which the view through the

windscreen became obscured by ice gave a very good indication of how rapidly icing was taking place on the entire airframe during a penetration.

The ice depth accumulated during each penetration is given on Figs. 8A-G in the upper right hand corner of each figure. The subjective estimates of icing rates are given as LICE (light icing), MICE (moderate icing) and SICE (severe icing) along the 10 km elevation line on Figs. 8A-G.

5.2.4 Lightning

Lightning observations are included as part of Figs. 8A-G. These observations were made by the pilot in real time and are included because it is felt that the lightning activity in a thunderstorm has an effect on the cloud physics. Smith (1968) observed that the least hail came from thunderstorms with the most lightning. There is no device on the aircraft to routinely record lightning or to even record when the aircraft was struck by lightning (which occasionally occurred). The pilot merely makes a comment into the voice recording system whenever lightning is observed. Of course using this system all lightning in the vicinity of the aircraft is not observed and noted by the pilot during a penetration, but it is felt that a fair representation of lightning is noted and verbally recorded.

Lightning strikes the aircraft on its extremities quite often but to date has done no significant damage to the airplane. Project Roughrider aircraft (Miller, 1968) also experienced numerous lightning strikes and they too concluded that with proper precautions there was little danger of severe aircraft damage due to lightning. Following the 1972 season lightning rods (Fig. 11) were added to the airplane

extremities to decrease any possible damage to the airframe, but no method of protecting the propeller has yet been devised.

The aviation fuel in the tanks of the T-28 is at a temperature and pressure which is only just slightly in the explosive range should the tanks be hit by lightning (Appleman, 1971). Since the tanks are vented through a port on a flat surface beneath the wing, there is very minimal danger of fuel explosion as a result of a lightning strike.

5.3 Ground Based Radar Data

The radar data used in this study were all from the NHRE project radars. The data were extensively computer processed to produce the figures used in this study.

5.3.1 M-33

The M-33 track radar was used as a source of "X - Y" position of the T-28 during penetrations. These data were acquired in the form of plots from a normal "X - Y" M-33 plotter and furnished by the Desert Research Institute as a part of their contract with the NHRE.

Although the M-33 track radar has a 1.0° conical beam, the azimuth and elevation angles are accurate to about 0.2° since the beam is conically scanned during tracking. The pulse length is 75 m but since the range notch is also scanned, the accuracy is about 30 m (Booker et al., 1967).

Since the T-28 was equipped with an X-band transponder, the M-33 had no difficulty maintaining lockon in even the most intense areas of a thunderstorm.

A remote M-33 acquisition display was used to vector the T-28 through the hailstorms of interest. Both the returns from the storms and the aircraft transponder were displayed on this scope for reference

during T-28 vectoring. The 5 1/2° vertical beam width of the M-33 acquisition radar did not give adequate vertical resolution to assure that the T-28 was being vectored through the desired level in the storm.

5.3.2 CPR-2

The other source of radar data was the CPR-2 radar belonging to the National Center for Atmospheric Research (NCAR) and operated by NHRE as the primary data acquisition radar system on the NHRE project. Eccles (1973) describes the radar and lists the radar parameters as given in Appendix A.

The CPR-2 was used to scan the entire cloud being penetrated by the T-28. The storm being penetrated was scanned using a zig-zag scan pattern up and down through the cloud. The normal procedure was to scan the entire cloud volume with the 1° conical beam. The time required to scan the entire cloud was usually about five minutes but varied substantially with distance from the radar. The greatest time required to scan the cloud occurred when the storms were closest to the radar. The data were recorded on magnetic tape so that later computer analysis was possible. The CPR-2 radar data were not available for real time display use by meteorologists at the Grover field headquarters.

According to a NHRE report *all the radar data gathered in 1972 had a consistent error of from -8 to -10 dBz. Accordingly 10 dBz were added to all the reflectivity* values recorded during the 1972 field season and used in this study. These values may still be in error, but they are based on the best calibration data currently available.

*The National Hail Research Experiment Summer 1973 Summary Report, Dec. 1973: NHRE Data Report No. 73/2, 93 pp.

*This term "radar reflectivity or reflectivity" will be used instead of "equivilant radar reflectivity factor level" when referring to dBz in the remainder of the paper.

The addition of 10 dBz seems to be more in keeping with values obtained from other studies of hailstroms (Chisholm, 1969; Dennis et al., 1971).

5.3.3 CAPPI Displays

The recorded radar data were processed after the field season at the NCAR computer facility to produce on microfilm the two kinds of displays used in this study to compare high reflectivity zones with observations made by the T-28 system and the pilot. The computer-derived displays consist of CAPPI displays and vertical sections along the track of the T-28.

A computer program was written by NHRE staff to produce CAPPI displays at each whole kilometer, MSL from the surface to the top of the radar detectable cloud as determined from the recorded CPR-2 radar reflectivity data. CAPPI's were generated by the computer along the T-28 path to show horizontal radar reflectivity at the level of the thunderstorm being penetrated. CAPPI's bounding the volume penetrated by the T-28 are shown in Figs. 9A-G. The CAPPI's are included to depict the T-28 track in relation to the horizontal dimension of the high reflectivity zones.

The ground track of the T-28 is superimposed on these figures. At one point on the track an "X - Y" coordinate is given in kilometers with respect to the Grover radar site, where +Y is true north and +X is east. The overall geographic reference system can be seen in Fig. 2. Two times are listed on each CAPPI corresponding to a known T-28 position at that time. Time ticks are plotted along the track at one minute intervals and correspond to whole minutes.

It can readily be seen from these CAPPI's that in most cases the T-28 was vectored through the areas of highest reflectivity in the storms of interest.

5.3.4 Vertical Sections

A computer program was written by a member of the IAS staff to display a vertical profile (along the T-28 track) of the thunderstorm being penetrated. The computer program used data recorded by the CPR-2 radar to display the reflectivity factor level values closest to a vertical surface which passes through the T-28 track. The reflectivity factor level values were printed to the nearest dBz in an array using altitude as the ordinate and time as the abscissa. Since the T-28 did not travel at a constant velocity there is no absolute relationship between time and distance. The aircraft did, however, travel at nearly a constant average velocity of 100 m sec^{-1} (200 kts) so this value can be used to approximately relate time and distance.

The vertical sections have the aircraft in the vertical plane depicted as a solid line. The individual data points were plotted each 500 m (1,640 ft) in the horizontal and each 1° elevation. They were then hand contoured to give the displays in Figs. 8A-G.

Due to the time required to scan a given cloud the computer program was written so that the times of the actual values printed on the vertical sections may differ by as much as 5 minutes from the times when the aircraft passed over or under these points. This usually provided a data point to fill that point in the array. Occasionally no data existed within $\pm$ 5 minutes of aircraft passage. Normally, however, a scan took about five minutes so the data points were within 2 minutes of the specified time from the aircraft track.

Figs. 8A-G

Caption for all vertical section, aircraft data and pilot's comments figures.

The vertical sections are hand contoured at 5 dBz intervals from computer generated reflectivity arrays. The outer contour represents 40 dBz. The vertical section is taken along the aircraft track as derived from the M-33 track radar. The aircraft path in the vertical plane is given. Turbulence values are given along the top of the figure with M and S representing areas of moderate and severe turbulence respectively.

Icing and lightning observations by the pilot are included along a line at the 10 km level. LICE, MICE and SICE represent light, moderate and severe icing respectively. The total airframe ice accumulated during a penetration is given at the far right along the 10 km elevation line. Lightning observations are marked with LTNG.

Hail encounters are indicated along the aircraft track by a hatched area.

The lower part of each figure represents aircraft data and was computer plotted. Traces of updraft velocity (m sec^{-1}), altitude (km) and JW LWC (g m^{-3}) are indicated by circles, squares and triangles respectively.

Time on the upper part of the figure references the true airspeed of the T-28 during a penetration while in the lower part of the figure time is plotted assuming a constant true airspeed of 100 m sec^{-1} (200 kts). This accounts for the slight abscissa discrepancy between the upper and lower parts of the figure.

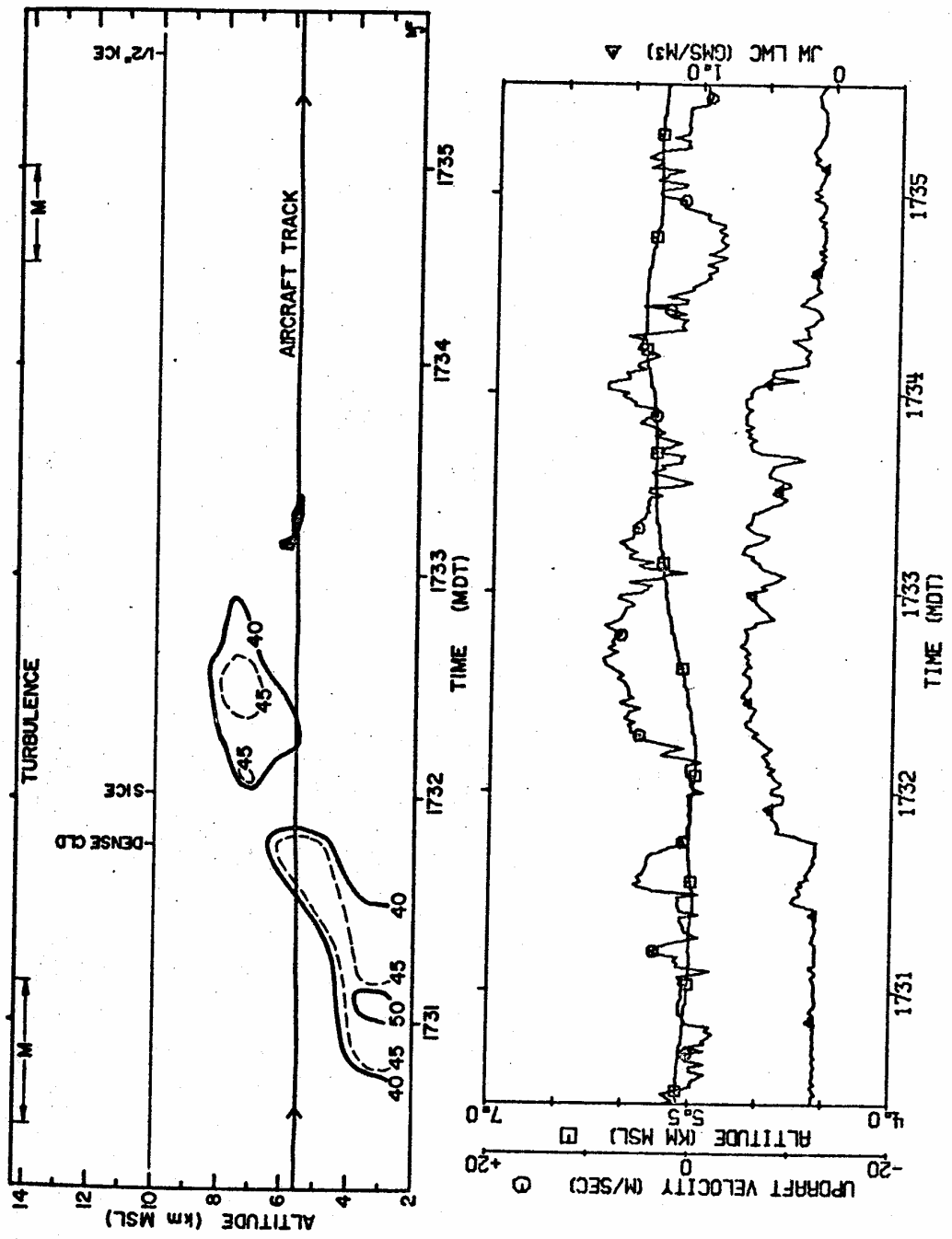

Fig. 8A. 21 June-Penetration 1. Vertical section, aircraft data and pilot's observations.

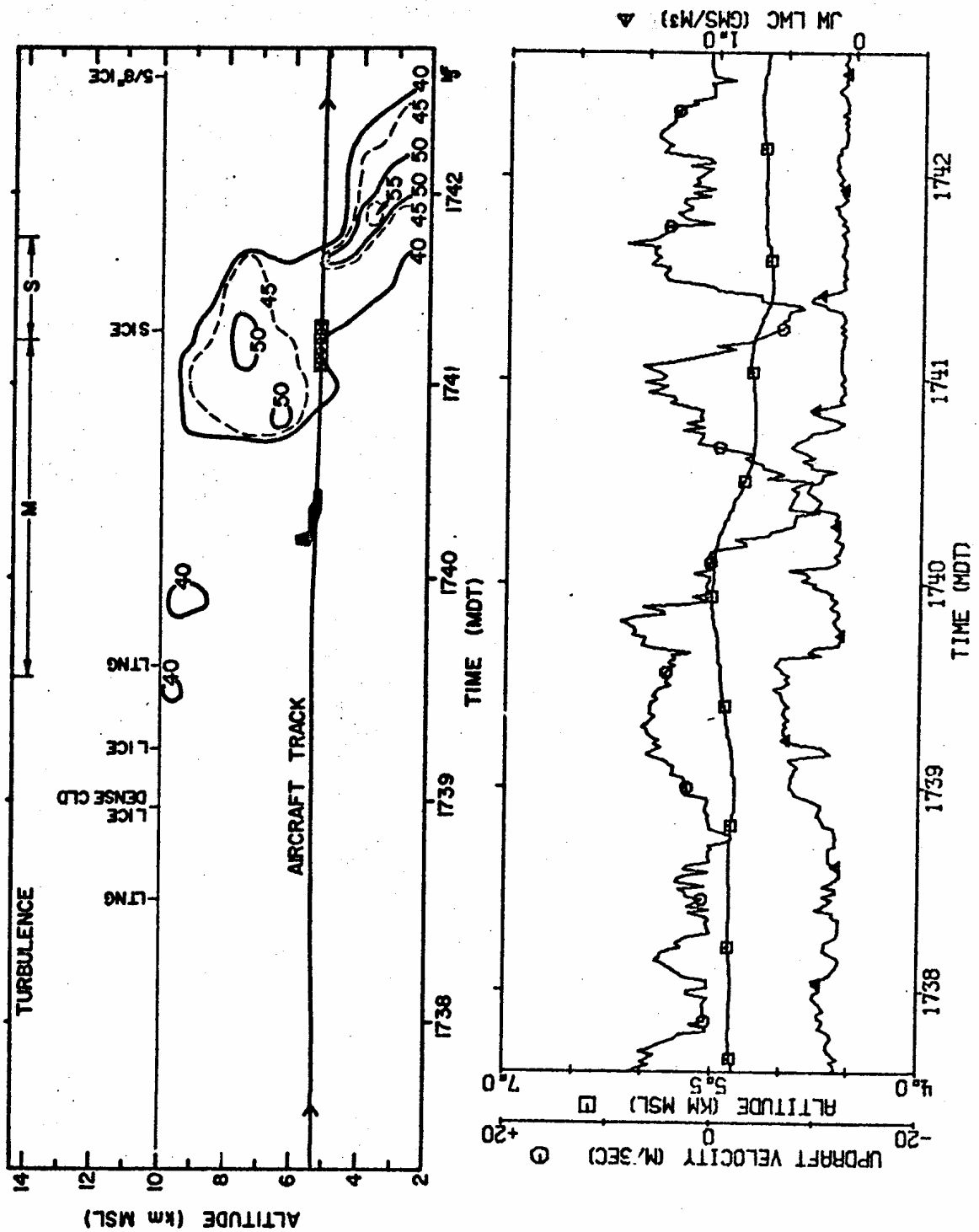

Fig. 8B. 21 June-Penetration 2. Vertical section, aircraft data and pilot's observations.

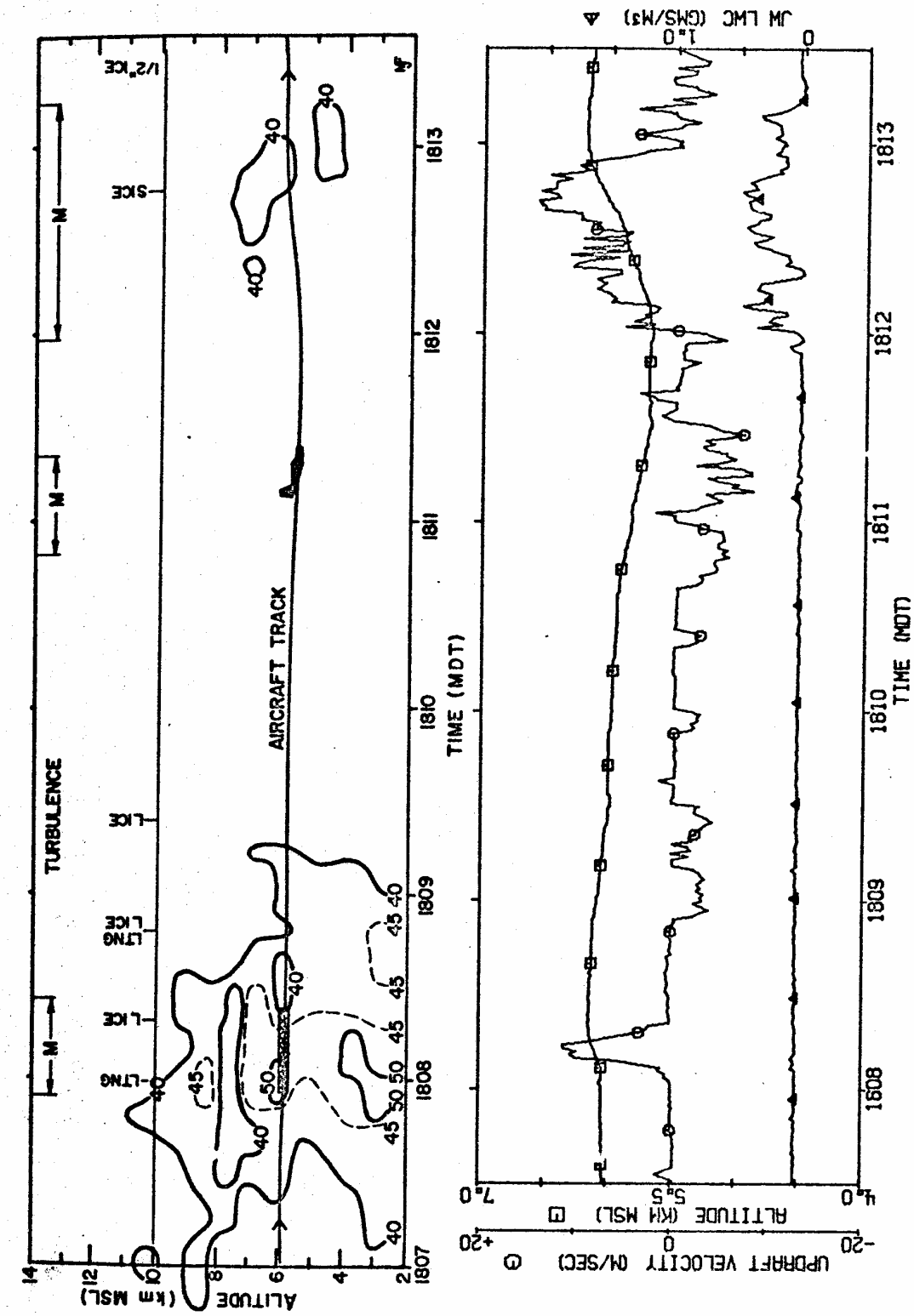

Fig. 8c. 7 July-Penetration 1. Vertical section, aircraft data and pilot's observations.

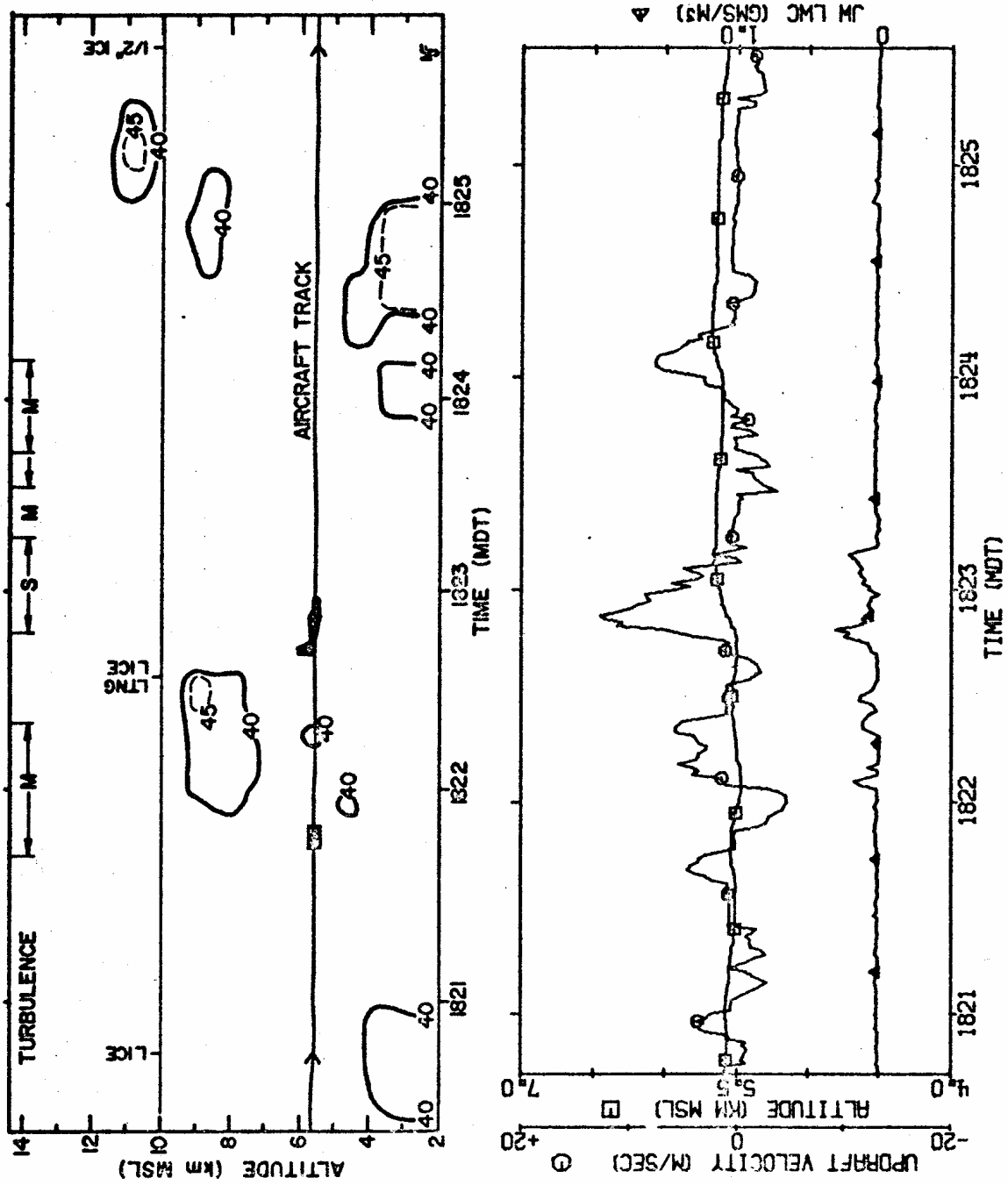

Fig. 8D. 7 July-Penetration 2. Vertical section, aircraft data and pilot's observations.

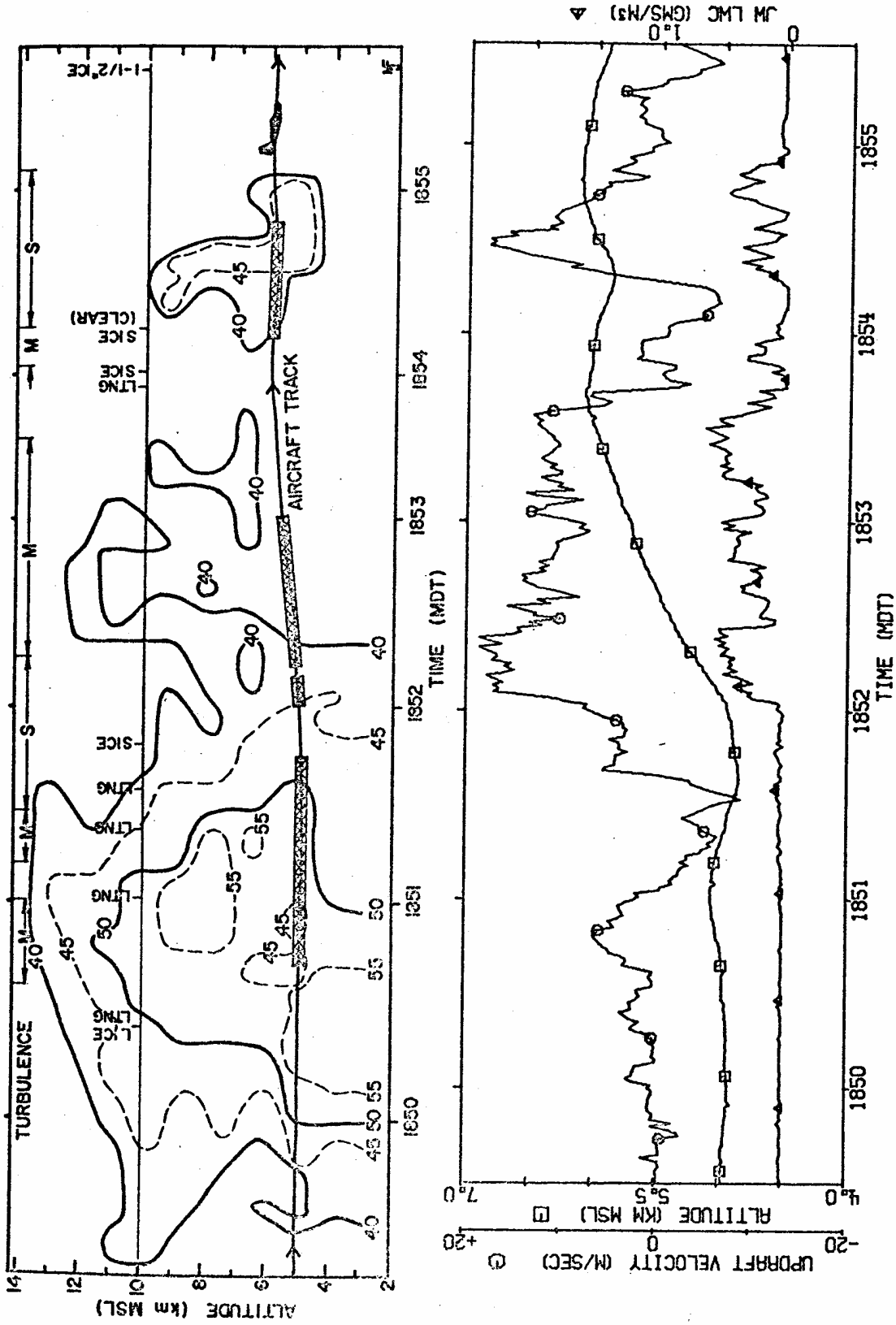

Fig. 8E. 7 July-Penetration 4. Vertical section, aircraft data and pilot's observations.

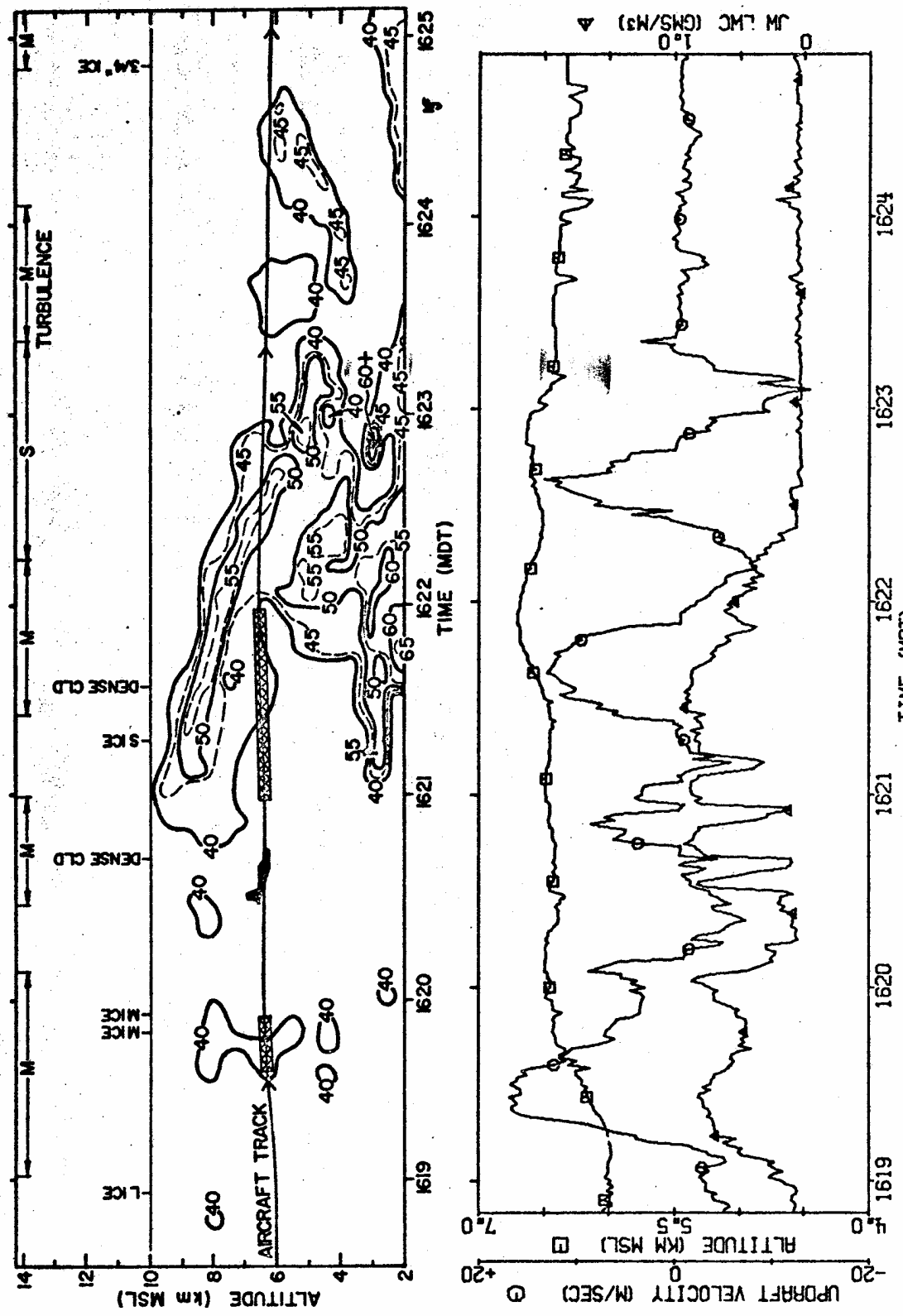

Fig. 8F. 22 July-Penetration 2. Vertical section, aircraft data and pilot's observations.

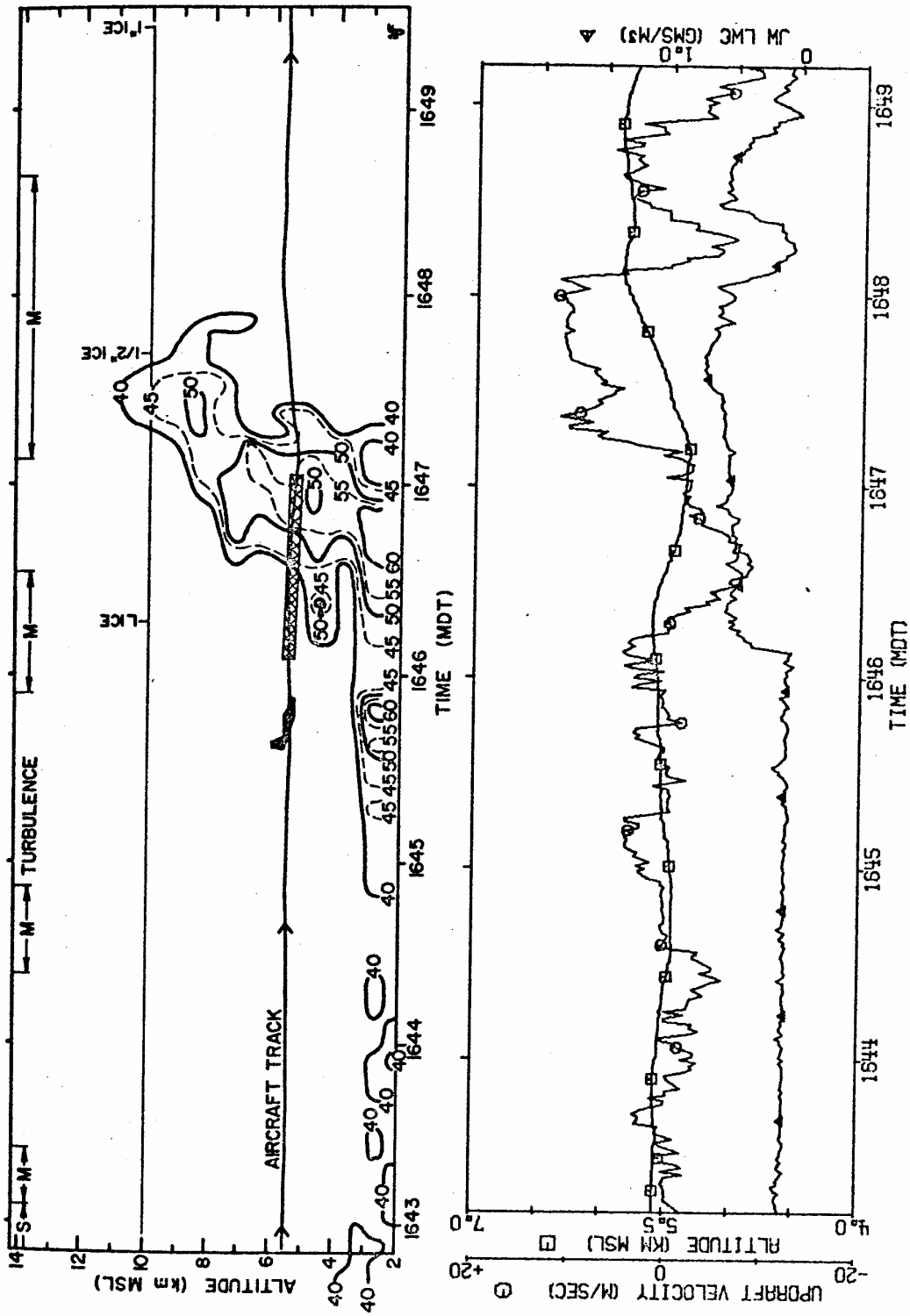

Fig. 8G. 22 July-Penetration 3. Vertical section, aircraft data and pilot's observations.

Figs. 9A-G

Caption for all CAPPI figures.

CAPPI's are machine contoured at 5 dBz intervals with the outer contour representing 40 dBz. Computer derived points of maximum reflectivity are noted with an "H". CAPPI's are given for whole km altitudes MSL such that they bracket the altitude of T-28 penetration. The T-28 track through the storm is given on each CAPPI. The times of two known locations are given to the second and tick marks are placed along each track representing whole minutes. A reference point on the track is given relative to the Grover radar site with +X representing east and +Y representing true north. These locations may be referenced to Fig. 2. Direction of storm motion is given by the arrow at the base of the true north arrow.

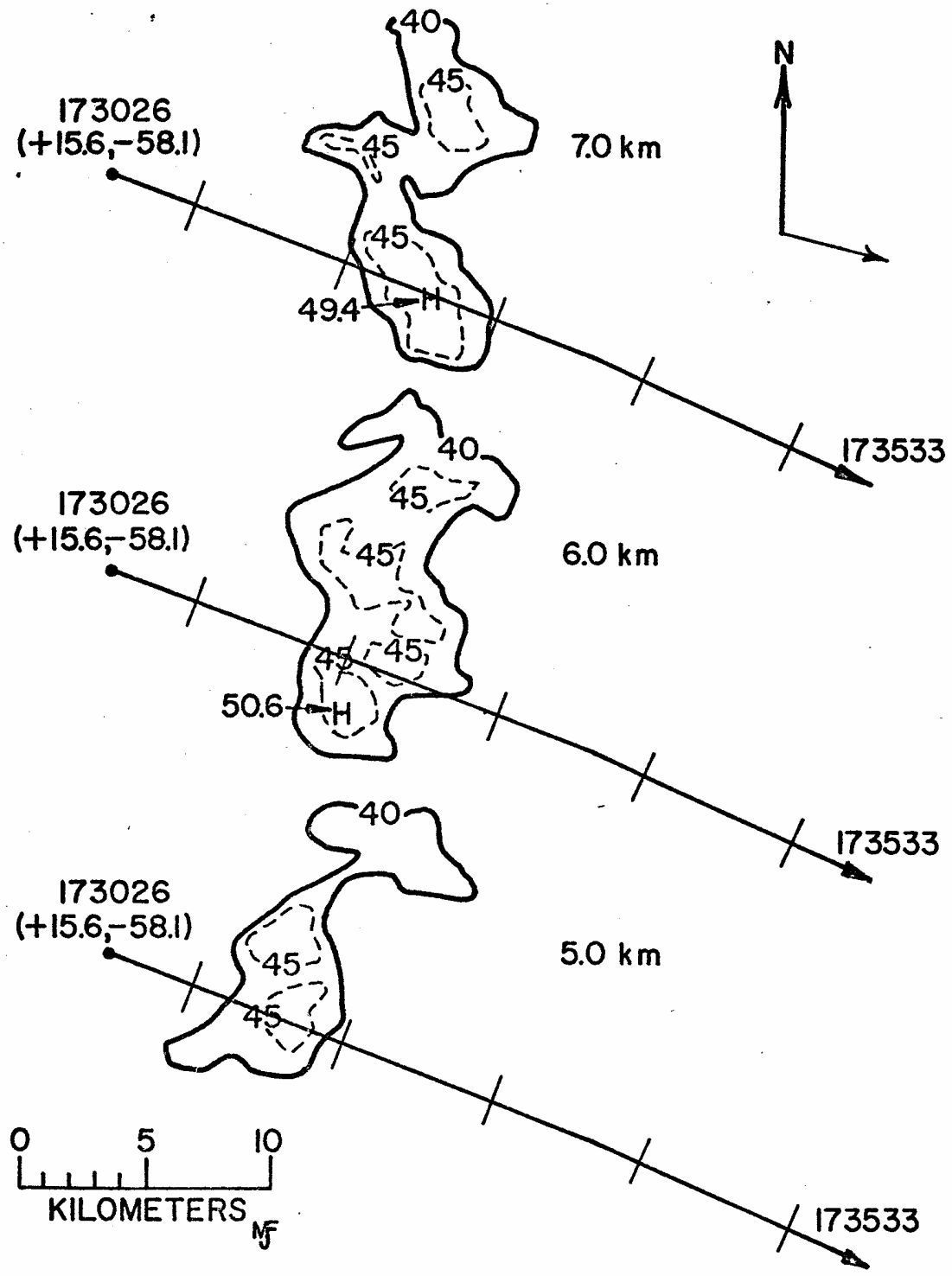

Fig. 9A. 21 June-Penetration 1. CAPPI displays at 5, 6 and 7 km MSL along T-28 track.

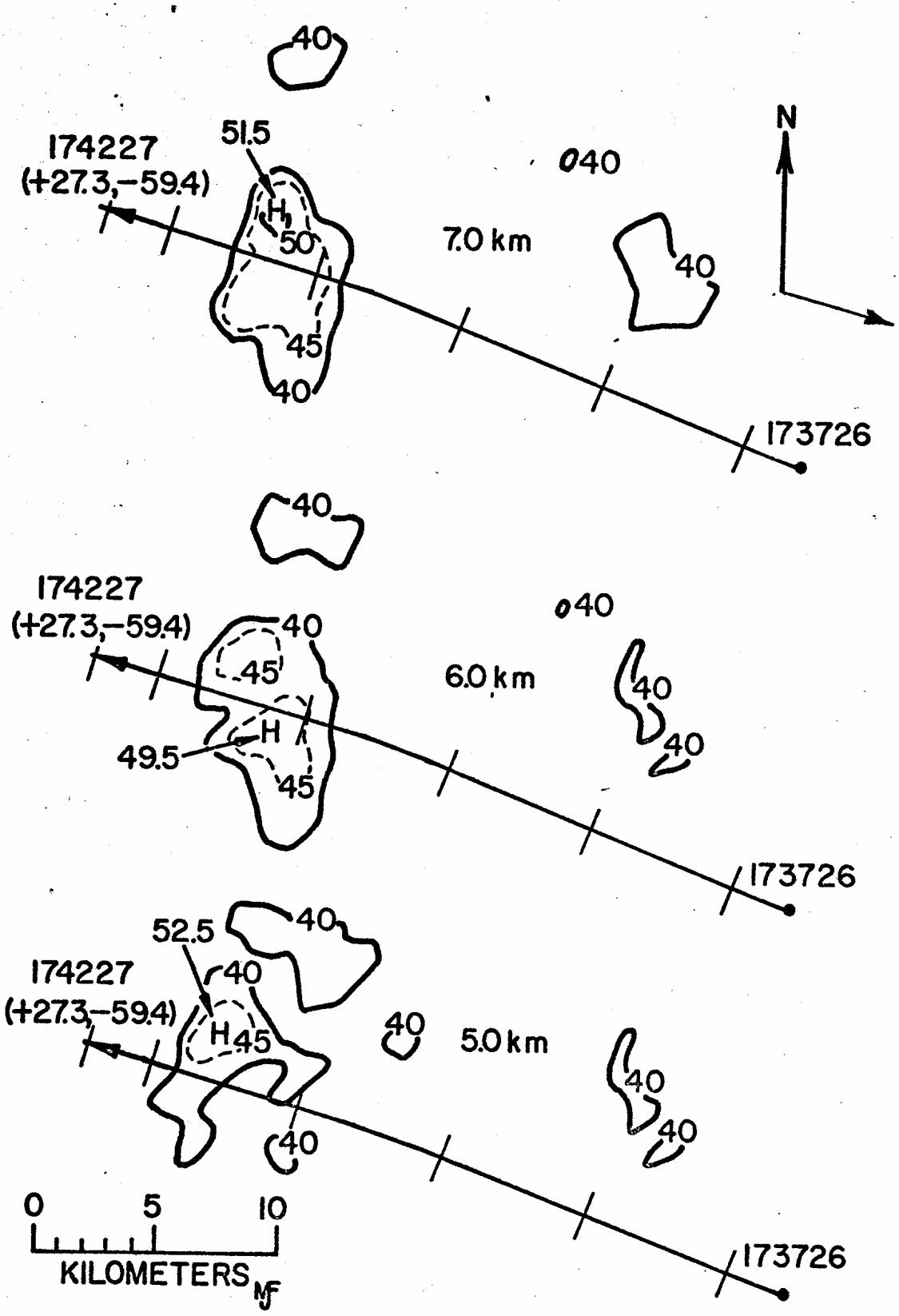

Fig. 9B. 21 June-Penetration 2. CAPPI displays at 5, 6 and 7 km MSL along T-28 track.

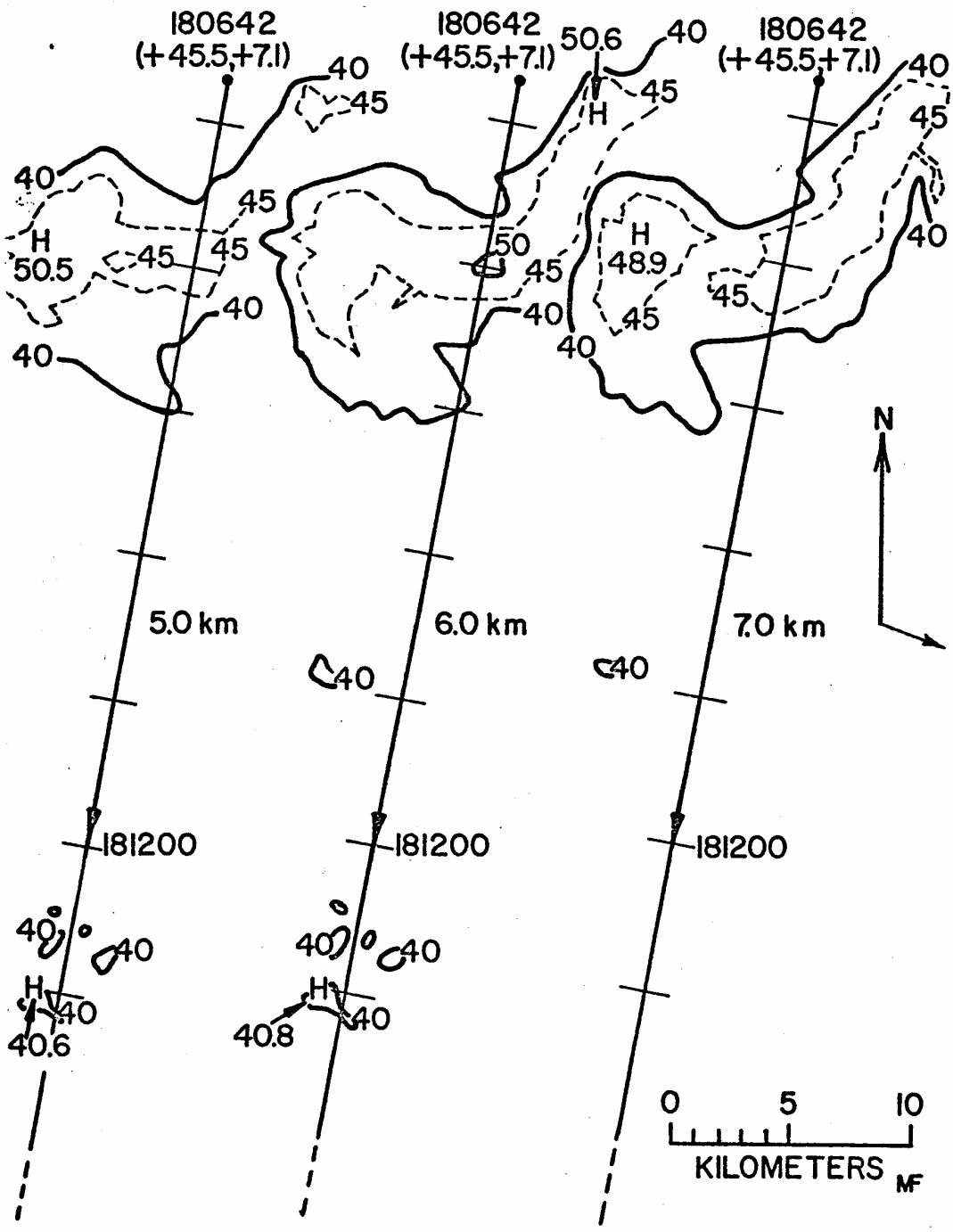

Fig. 9C. 7 July-Penetration 1. CAPPI displays at 5, 6 and 7 km MSL along T-28 track.

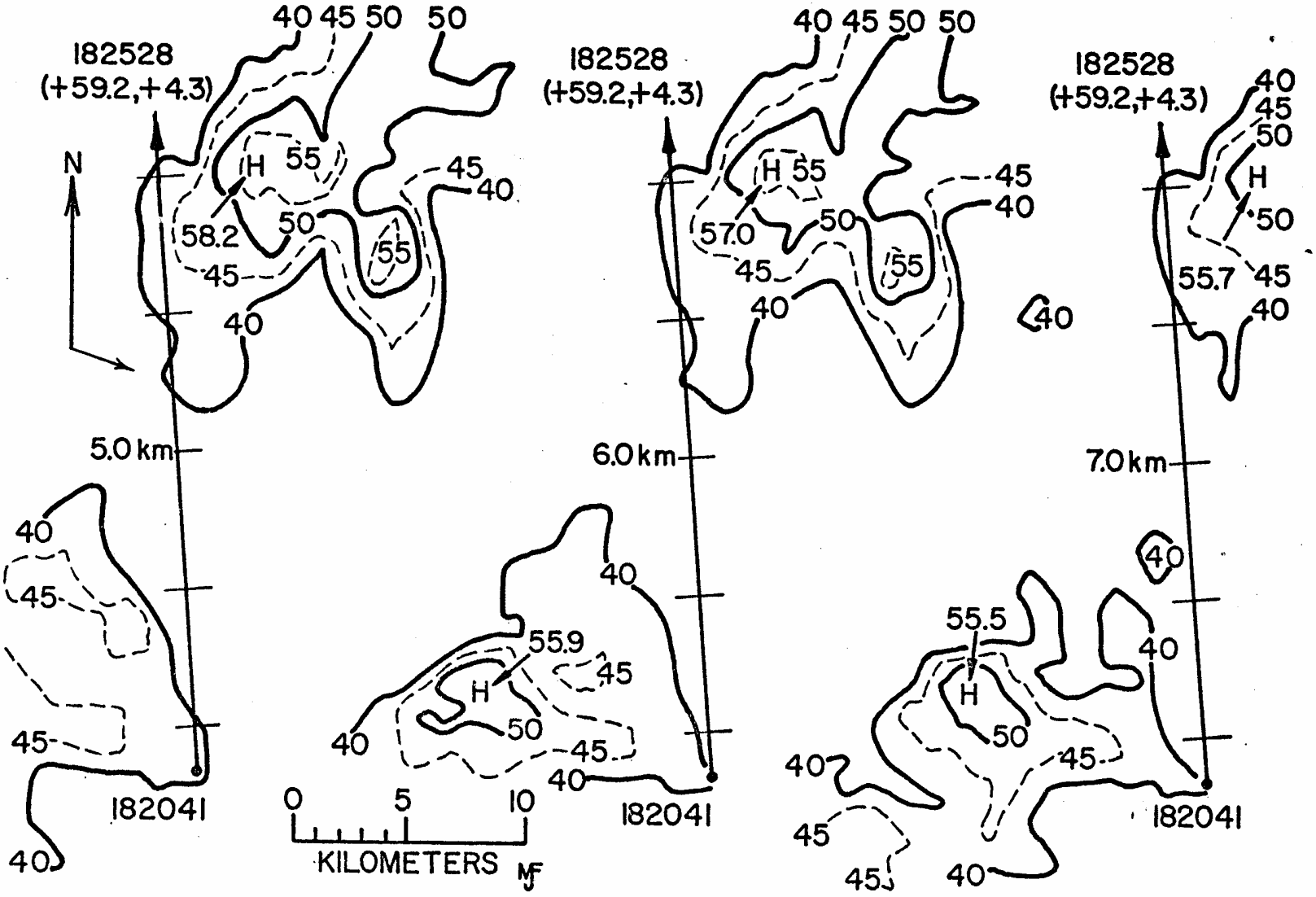

Fig. 9D. 7 July-Penetration 2. CAPPI displays at 5, 6 and 7 km MSL along T-28 track.

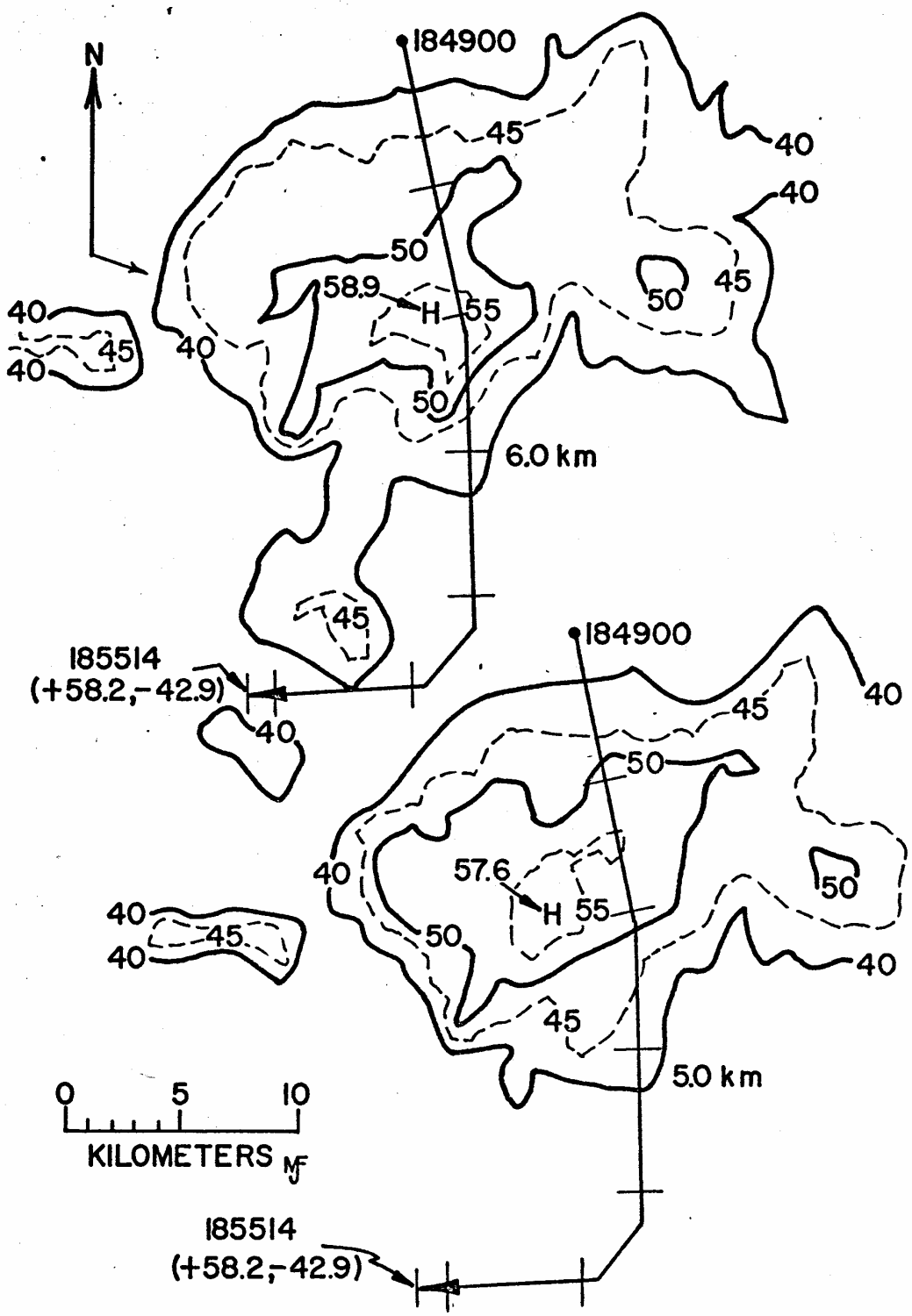

Fig. 9E. 7 July-Penetration 4. CAPPI displays at 5 and 6 km MSL along T-28 track.

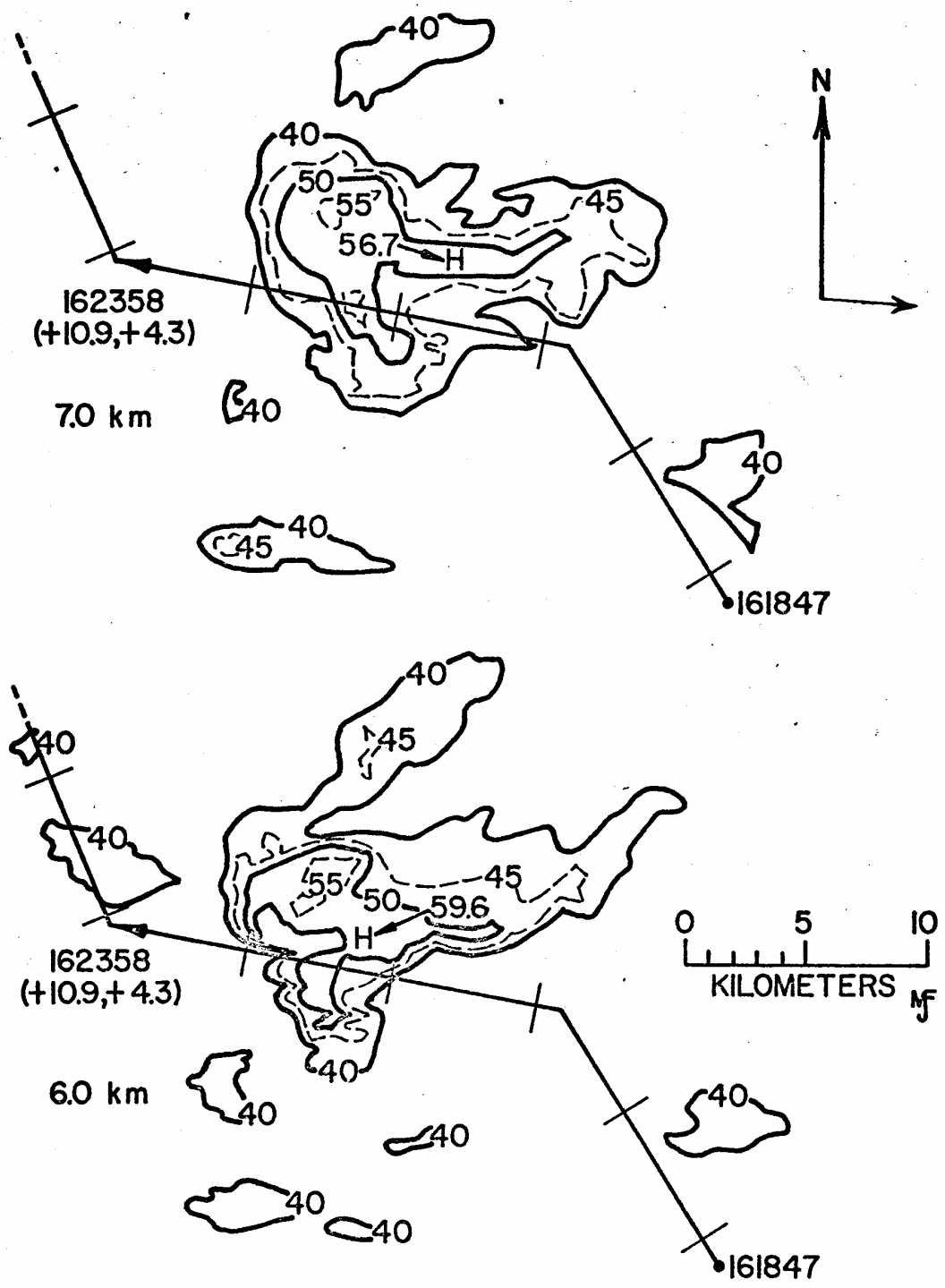

Fig. 9F. 22 July-Penetration 2. CAPPI displays at 6 and 7 km MSL along T-28 track.

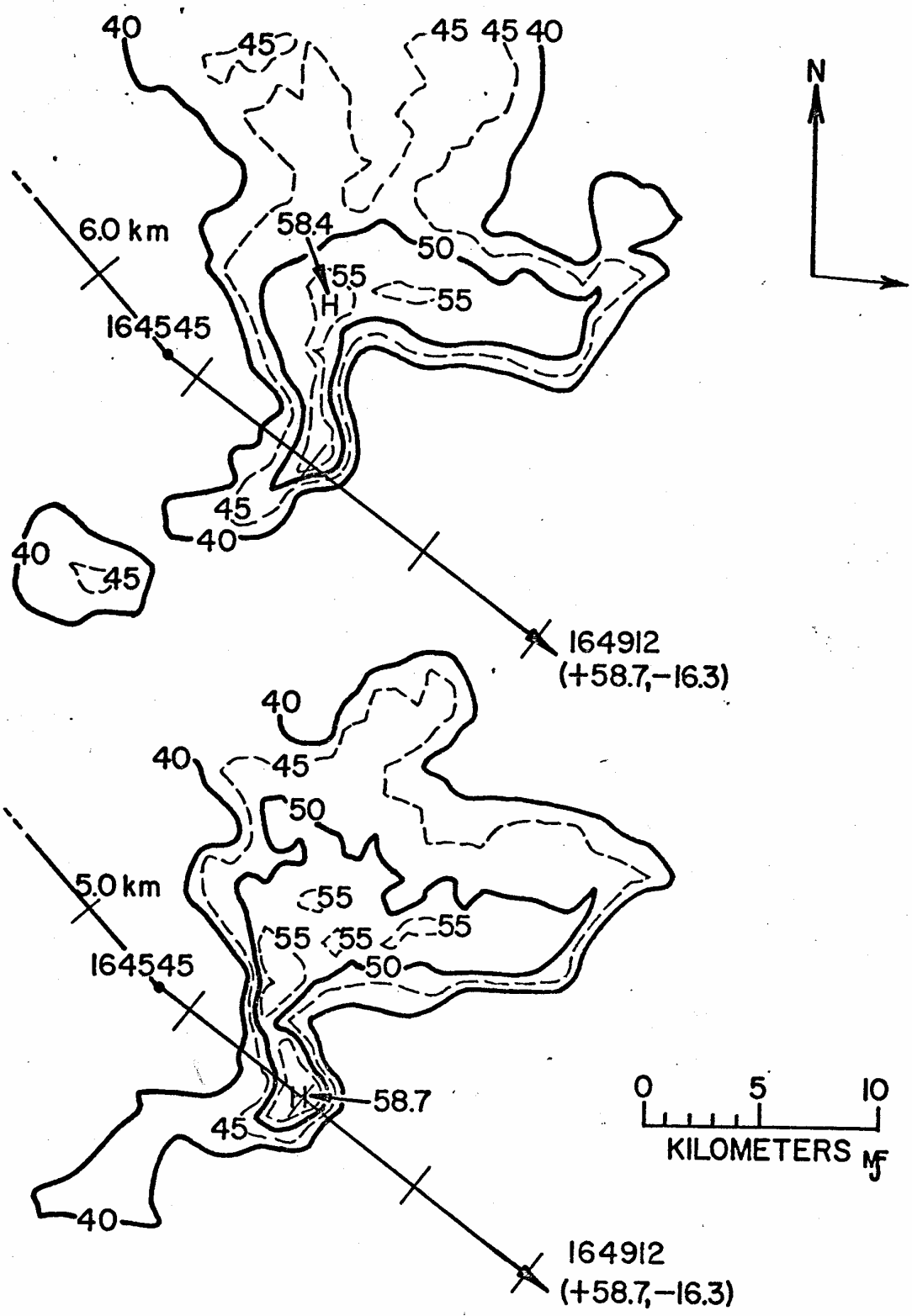

Fig. 9G. 22 July-Penetration 3. CAPPI displays at 5 and 6 km MSL along T-28 track.

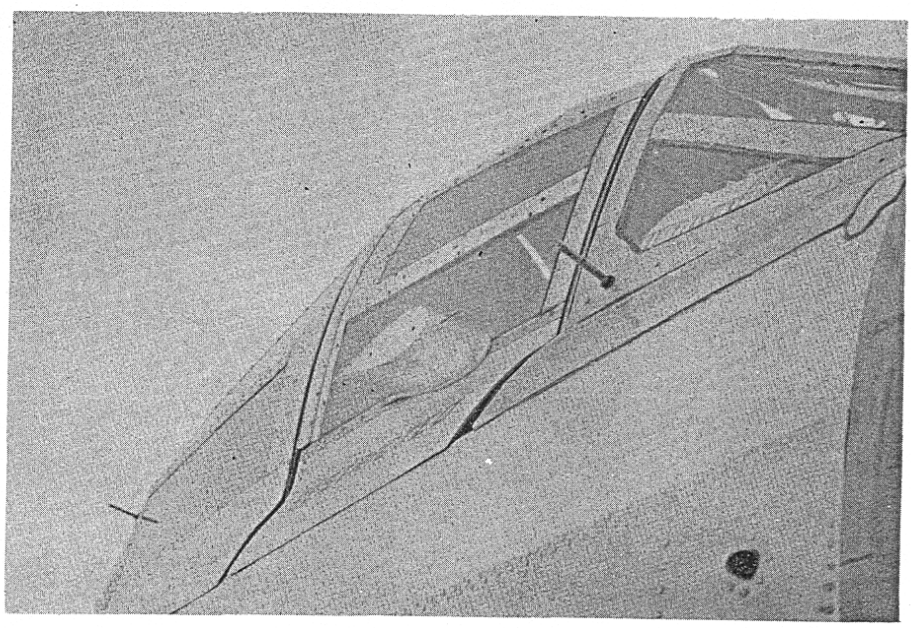

Fig. 10. Ice depth probe. The graduated rod on the small airfoil enables the pilot to visually determine the depth of ice on the aircraft.

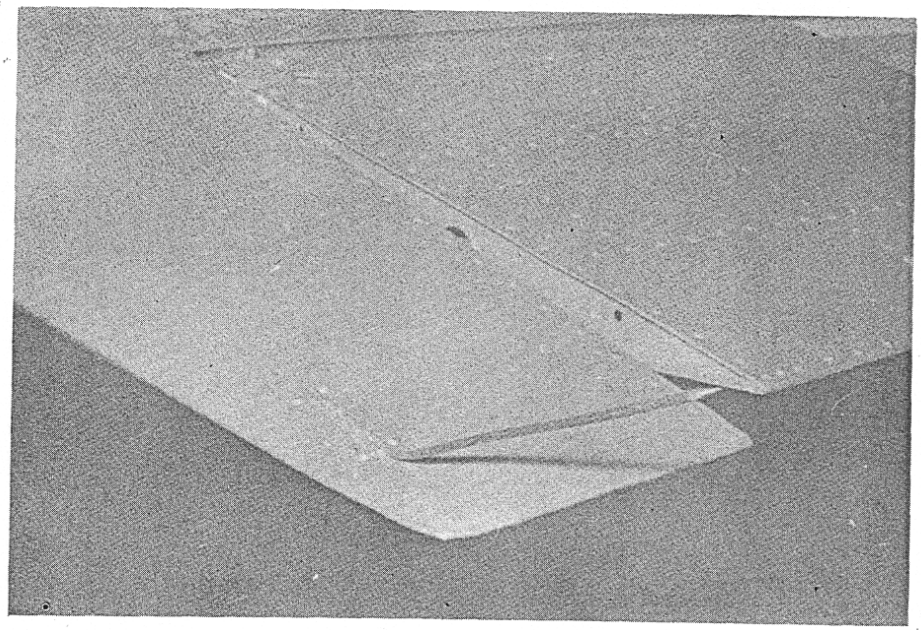

Fig. 11. Lightning rods mounted on all T-28 airfoil tips.

6. HAILSTORMS PENETRATED

The seven penetrations studied in this thesis were made on three separate days. The penetrations will be referred to by date and penetration number, i.e., 21 June-2 would indicate the second penetration on 21 June. All penetrations were made in 1972, so no year will be included in this method of identifying individual penetrations.

It is beyond the scope of this study to discuss causes of thunderstorms or even describe in detail the synoptic situation on the days which produced the thunderstorms that were penetrated. Even so a brief description of certain aspects of each day under study is felt to be in order.

A sounding from a station located in the inflow region of the thunderstorm at or near the time of the penetration is included as Figs. 12, 14 and 16 for each of the days on which penetrations were made. A hodograph is also included for each of the days (Figs. 13, 15 and 17). All three of the hodographs presented here have characteristics of supercell storms as described by Marwitz (1972a).

Details on the exact times of visual cloud entry and exit plus the times of radar echo entry and exit are given in Table 2. Also included is an estimated mean hail size and a duration time of hail encounters for each of the seven penetrations.

6.1 21 June 1972

There were numerous thunderstorms in the area throughout the afternoon on this day with significant development beginning by 1325 MDT. Golf ball sized hail was reported in Northeast Colorado on this day but no significant hail was reported in the NHRE operations area (Fig. 2). It can be seen from the hodograph (Fig. 13) that considerable shear was

present. By mid afternoon all the soundings in the area were similar to the one shown in Fig. 12, which indicates an unstable atmosphere. The storm penetrated was outside the NHRE hail observation network so no surface hail data are available from this storm.

6.2 7 July 1972

Only two major cells developed in the NHRE operations area (Fig. 2 on 7 July. These two cells were quite severe and produced significant amounts of hail all across the network and the protected area. A funnel cloud was sighted by a surface observer just west of Sterling, Colorado and very near the area where the T-28 made penetration number four on this day.

As can be seen from the hodograph (Fig. 15) and the sounding (Fig. 14) this was an unstable day but with considerably less shear and lighter winds aloft than on the other two days used in this study. It should also be noted that the storms on 7 July had higher tops than did the storms on the other two days used in this study.

Hail as large as marble size was reported on the surface and was observed during penetration 4. The largest quantity of hail encountered on any single penetration during 1972 occurred during penetration 4.

6.3 22 July 1972

The storm penetrated on 22 July has been the subject of considerable study by NHRE participants (Musil et al., 1973; Fankhauser and Foote, 1973; Bushnell, 1973; Phillips, 1973 and Sand et al., 1973). The storm penetrated developed in mid afternoon after another smaller storm had passed through part of the NHRE operations area in the early afternoon. Considerable shear is evident in Fig. 17. Hail up to about 1.9 cm (3/4 in) diameter was observed during the third penetration on this day

to mark the largest hail observed in cloud during the 1972 season. Visually the storm was not impressive because of its relatively low tops. Only sparse amounts of hail were observed at the ground. The largest stone recorded in the network was approximately 1.5 cm (marble) diameter.

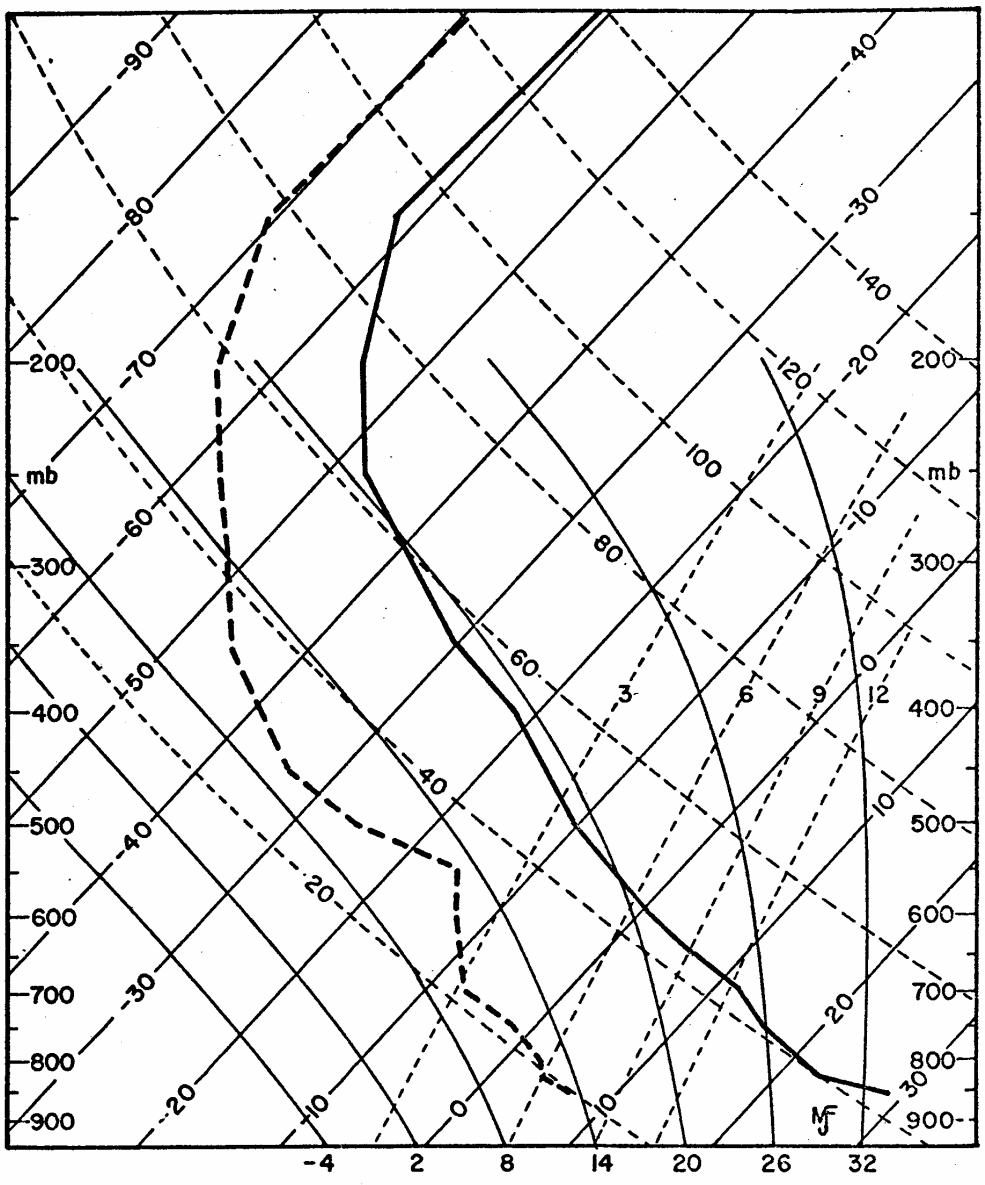

Fig. 12. 21 June 1972 - Sounding of temperature and dew point - Fort Morgan 1359. Skew T - Log p.

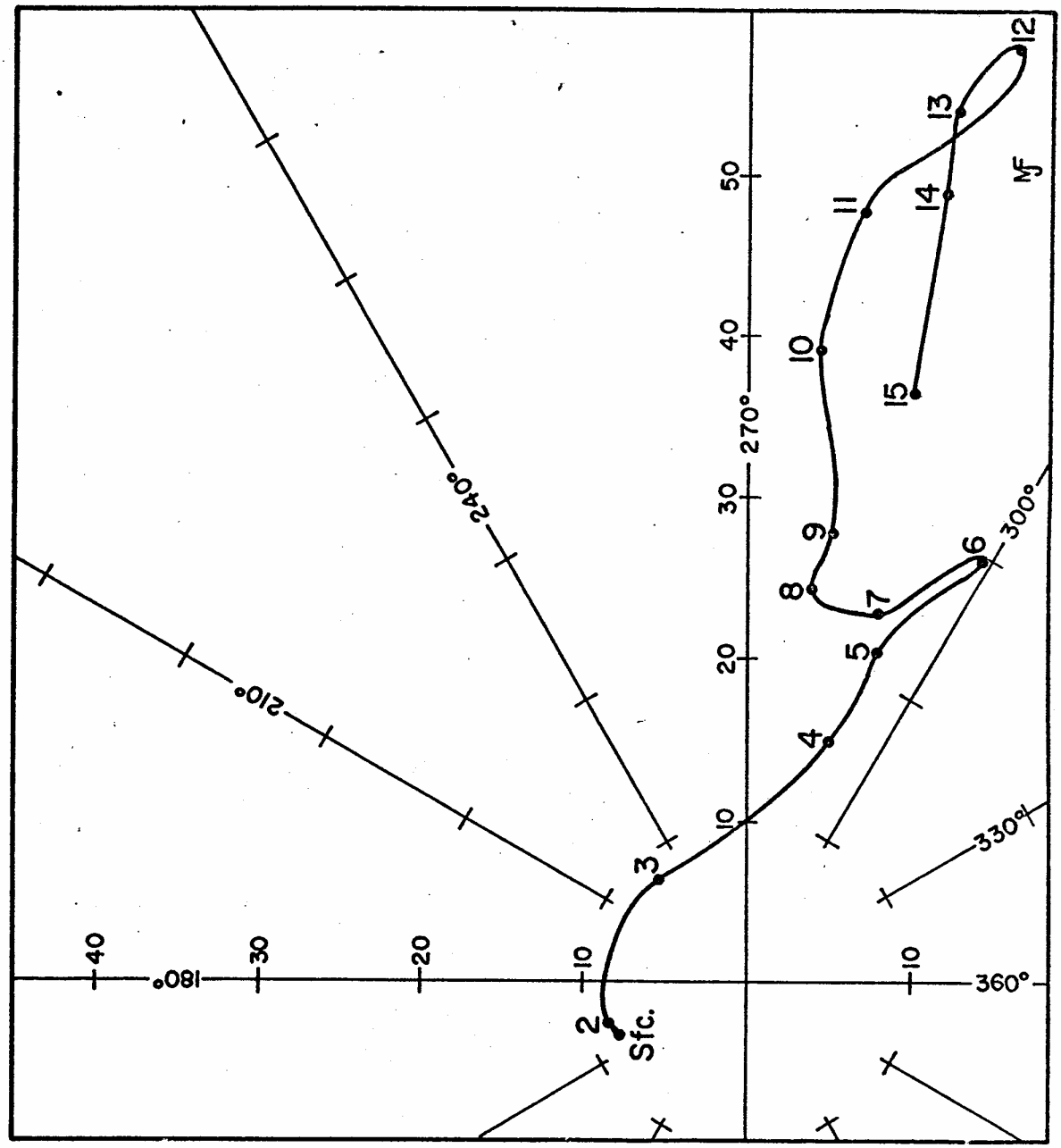

Fig. 13. 21 June 1972 - Hodograph - Fort Morgan 1359 MDT. Altitudes are in km MSL and velocities are in m sec^{-1}.

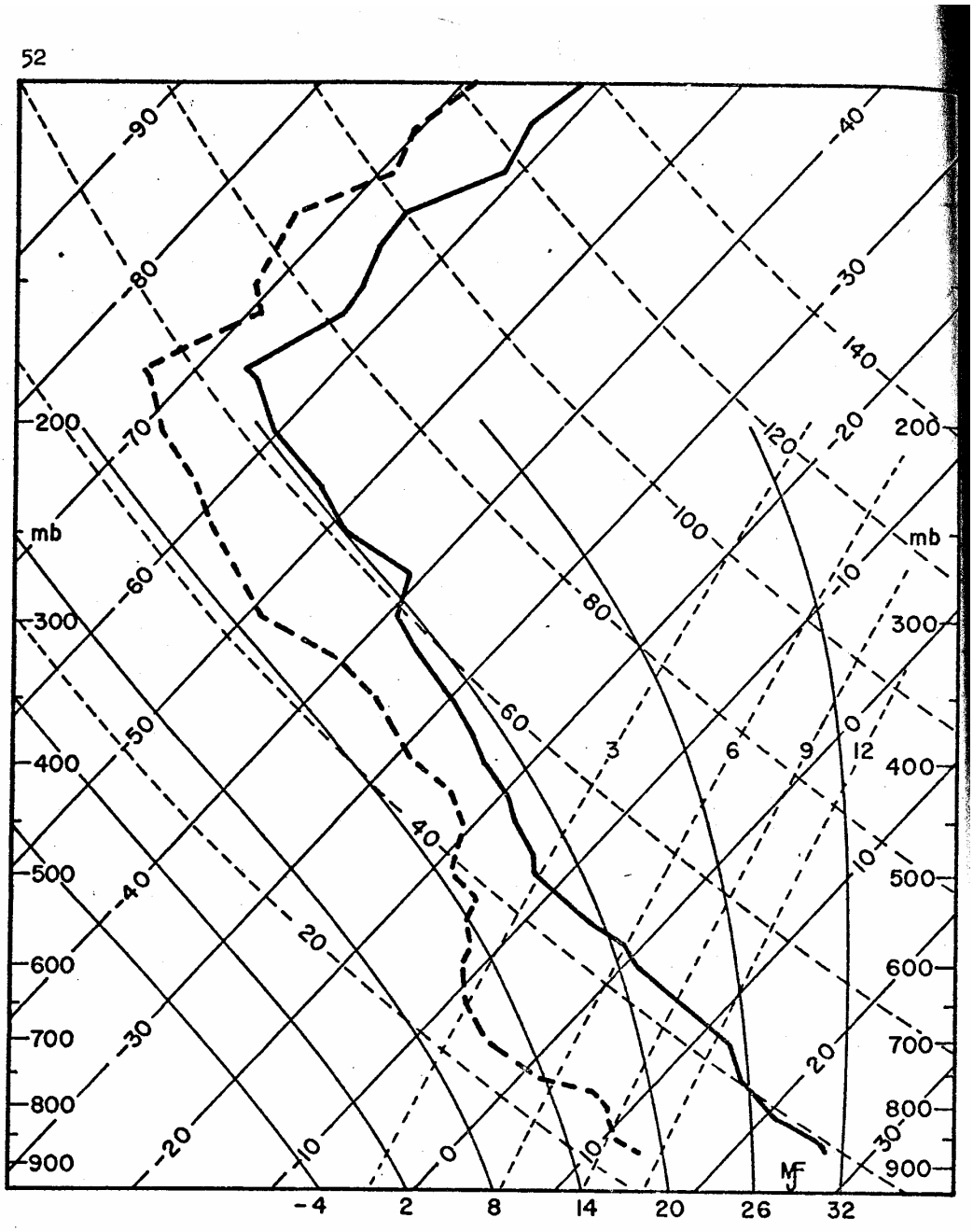

Fig. 14. 7 July 1972 - Sounding of temperature and dew point - Sterling 1651 MDT. Skew T - Log p.

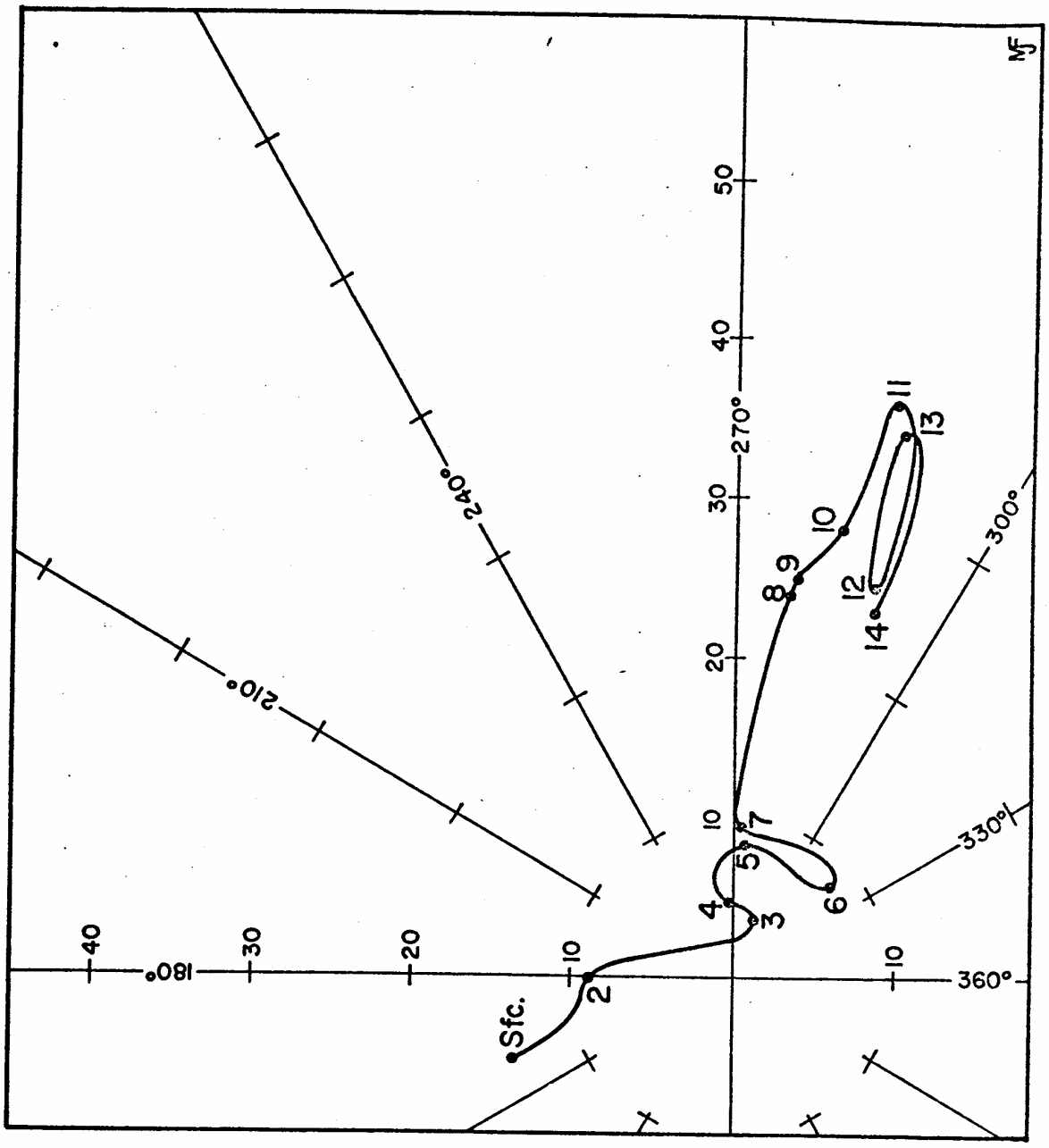

Fig. 15. 7 July 1972 - Hodograph - Sterling 1651 MDT. Altitudes are in km MSL and velocities are in m sec^{-1}.

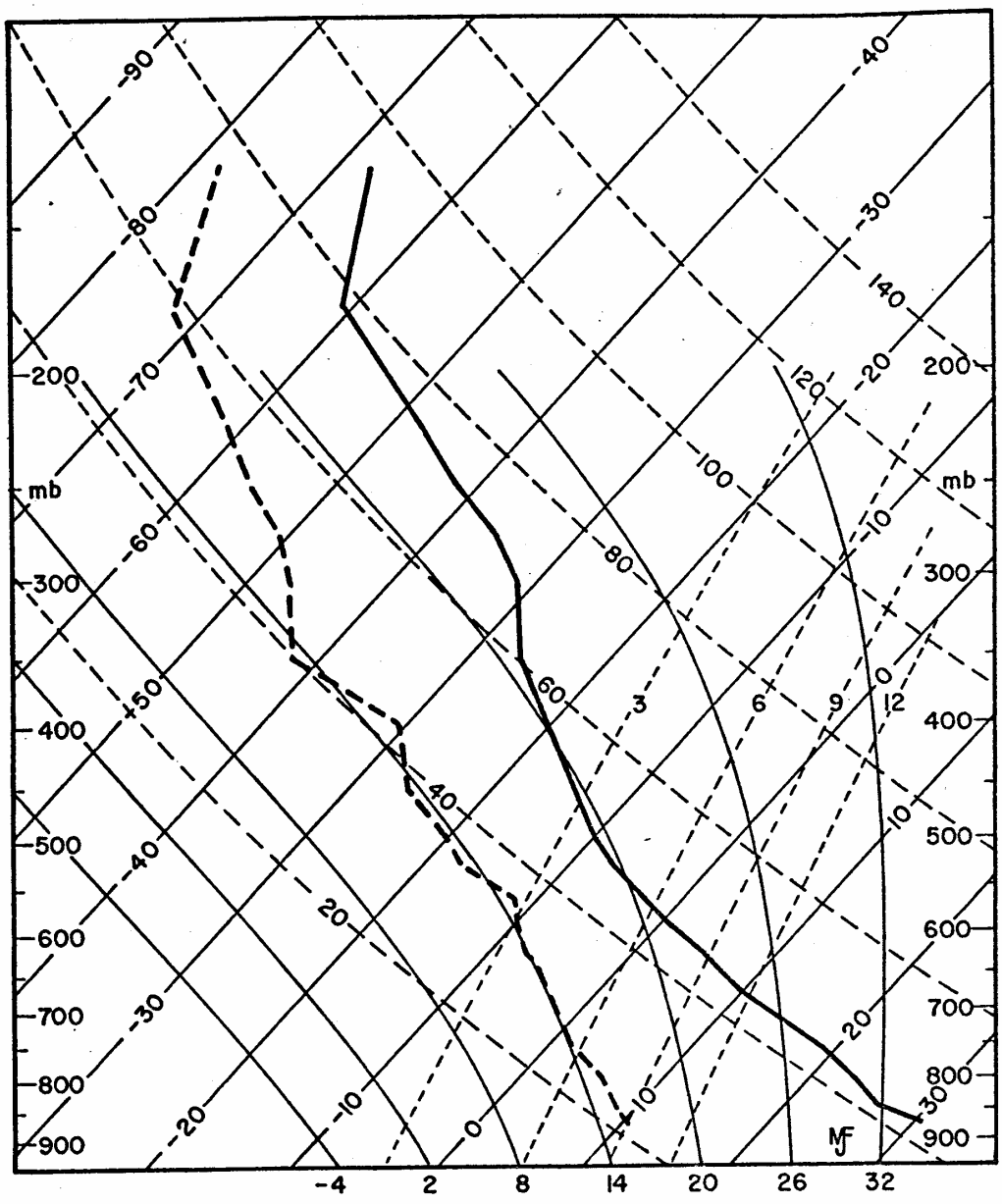

Fig. 16. 22 July 1972 - Sounding of temperature and dew point - Sterling 1650 MDT. Skew T - Log p.

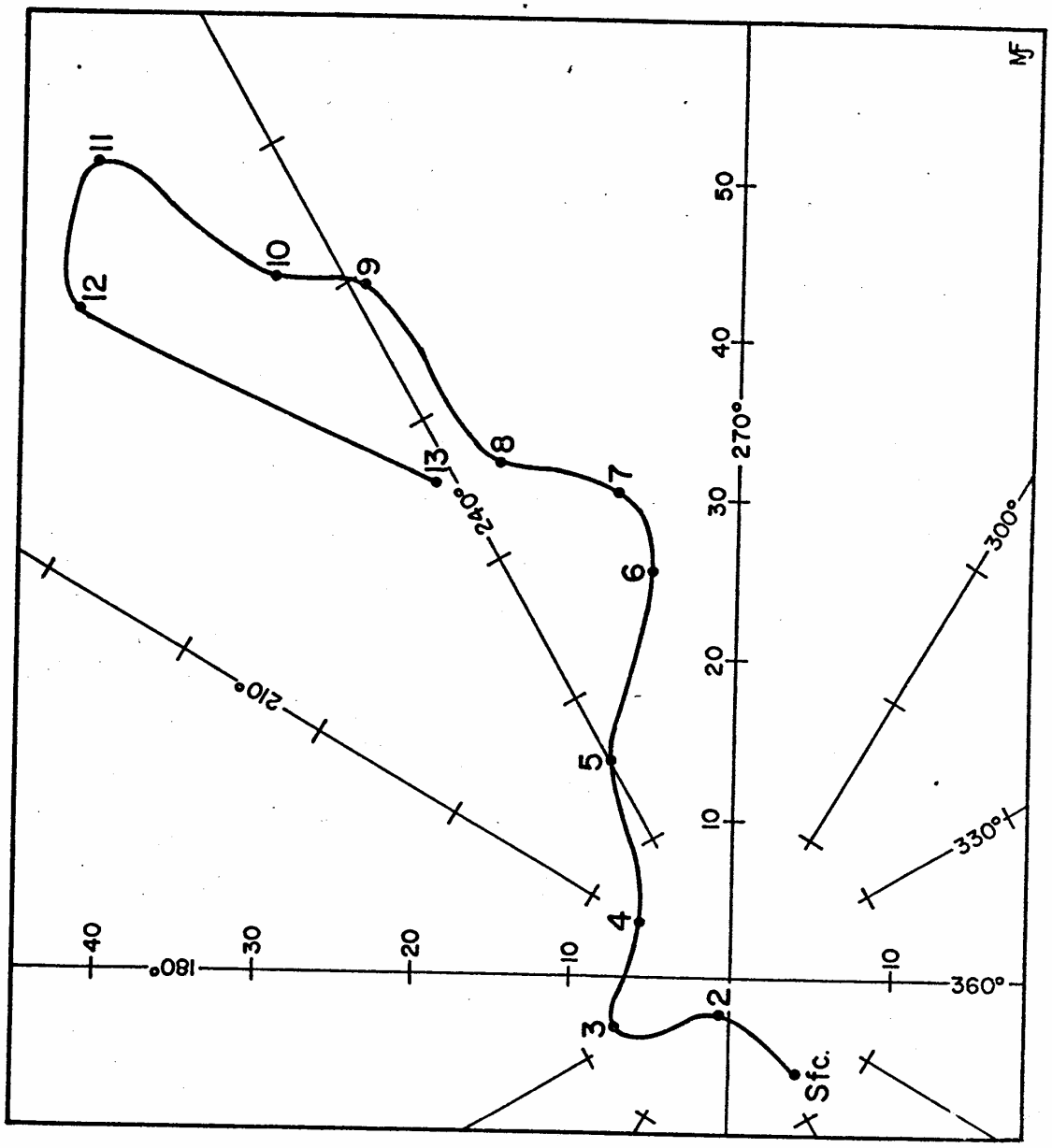

Fig. 17. 22 July 1972 - Hodograph - Sterling 1650 MDT. Altitudes are in km MSL and velocities are in m sec^{-1}.

Table 2

Summary of hailstorm penetrations

Date	Penetration	Visual Cloud		Radar Cloud		Altitude (km)		Hail			Average Temp. C
		Entry	Exit	Entry	Exit	Min	Max	Start	Duration	Size	
21 June	1	173026	173533	173048	173330	5.48	5.91	-	-	-	-10.5
21 June	2	173736	174227	174020	174210	5.09	5.53	174103	15 sec	Pea	-8.5
7 July	1	180642	181447	180643	181003	5.68	6.21	180756	26 sec	Pea	-12.0
7 July	2	182041	182459	182228	182528	5.47	5.68	182143	6 sec	Pea	-11.0
7 July	4	184932	185505	184900	185514	4.85	6.13	185040	62 sec	Marble	-7.5
								185201	9 sec	Marble	
								185213	48 sec	Marble	
								185413	26 sec	Marble	
22 July	2	161847	162936	162051	162558	5.97	6.70	161934	16 sec	Pea	-15.3
								162058	60 sec	Pea to Marble	
22 July	3	163900	164912	164155	164805	5.35	5.89	164605	57 sec	Pea to 19 mm	-9.0

7. DISCUSSION OF RESULTS

Only the major characteristics of hailstorms are described in terms of updrafts, JW LWC, turbulence, hail, icing and lightning. The high radar reflectivity zones are used as a reference point and all observations are made relative to these areas.

The high radar reflectivity zones have been determined with the NHRE CPR-2 radar and plotted as CAPPI's and vertical sections. The observed composition of hailstorms has been determined by the data acquisition system on the T-28 armored aircraft and by personal observations by the author while piloting this aircraft through the high reflectivity areas of hailstorms.

7.1 High Reflectivity Versus Updrafts

The thunderstorm penetrations discussed here are all felt to be at or very near the level in the thunderstorm containing the maximum vertical velocities. In all cases measured with chaff, the maximum vertical velocities were found between 4 and 8 km MSL (Marwitz, 1973). This height of maximum updraft is also reported by the Russians (Sulakvelidze et al., 1967). The Hirsch model (Hirsch, 1971) was used by Musil et al. (1973) on data from 22 July-3 and indicated that the maximum updraft should be found at about 6.5 km MSL (about 1 km above the penetration altitude).

It has become common in recent years to associate thunderstorm updrafts with the weak echo region, (Chisholm and English, 1973; Marwitz, 1972a, b and c; Marwitz and Berry, 1970; Browning, 1964, and Newton, 1963). Using radar as the primary measurement tool, it is only natural that such concepts should develop and persist. With no particles large

enough to give a radar return in the area ahead of *the high reflectivi zone it is impossible for radar to detect updrafts in the area.

Measurements have also been made at and near cloud base (Auer and Sand, 1966; Auer and Marwitz, 1968; Hart and Cooper, 1969; and Dennis et al., 1970) indicating that the inflow region is just ahead of the high reflectivity zones and that it persists in this area for long periods of time.

Since the cloud penetrations in the present study were made completely through the visual cloud and well above cloud base, areas of up drafts throughout the cloud were determined. When Figs. 8A-G and 9A-G are studied it is found that in fact updrafts do not always occur exclusively in the weak echo regions beneath higher reflectivity zones aloft in the thunderstorms studied. Only two of the cases studied actus ly had the major updrafts unquestionably located primarily in the weak echo region under the overhanging high reflectivity zones (penetrations 7 July-4 and 22 July-3, Figs. 8E and 8G). Penetrations 21 June-1, 21 June-2 and 22 July-2 (Figs. 8A, 8B and 8F) had updrafts that were in th weak echo region in addition to updrafts well ahead of the high reflect vity zones. Penetration 7 July-1 (Figs. 8C) had the major updraft in a area well ahead of the weak echo region and the high reflectivity zone. Penetration 7 July-2 (Fig. 8D) was made in the area between two echoes and did not penetrate the high reflectivity zones or the weak echo regions of either storm. In the case of 7 July-2 (Fig. 8D) the major updraft encountered appears to be along the edge of the inflow area. Severe turbulence noted there would tend to confirm that only the edge of a strong updraft was penetrated and only the shear zone was encountered

* "Ahead of" refers to downstream in the direction of storm motion.

The seven penetrations in this study seem to indicate that updrafts well above cloud base can be found in almost any area of the cloud. It has previously been noted (Musil, et al., 1973; and Sand et al., 1973) that multiple updraft areas were encountered during penetrations 22 July-2 and 22 July-3 (Figs. 8F and 8G). In other studies of this same hailstorm, (Phillips, 1973; Fankhauser and Foote, 1973) two updraft regions at cloud base were observed. These observations were based on dropsonde measurements (Bushnell, 1973), surface hail reports and airflow measurements made by aircraft circumventing the storm.

The major updrafts are frequently located in the weak echo region, but this is not necessary. The updrafts at penetration level are frequently found well ahead of the high reflectivity zones giving the impression that the inflow is in the process of shifting to another position and that the storm is propagating in a noncontinuous fashion rather than with the common steady state inflow characteristics observed at cloud base (Auer and Sand, 1966; Auer and Marwitz, 1968; and Marwitz and Berry, 1970). The concept of the updraft moving from under the high reflectivity areas aloft was suggested by Dennis, et al. (1970). They postulated that the sloping updraft and the rotating storm were two possibilities allowing the system to overcome the precipitation brake and continue as an active hailstorm.

This study would tend to indicate that a discontinuous updraft propagation is the most likely mechanism indicating a characteristic similar to the multi-cell storms described by Marwitz (1972b).

7.2 High Reflectivity Versus Liquid Water Concentration

Keeping in mind the limitations of the JW LWC device as discussed in section 5.1.4 a comparison can be made between the output of this

device and the high radar reflectivity zones by referring to Figs. 8A-G. It is readily apparent that the high radar reflectivity zones and the high readings on the JW LWC device do not coincide, the one exception being penetration 22 July-3 (Fig. 8G). In all other penetrations the JW LWC device indicated values very near zero in the high radar reflectivity zones.

It is also obvious from Figs. 8A-G that the high values of JW LWC correspond well with strong updrafts. This is interpreted as meaning that there are very few liquid cloud droplet sized particles in the high radar reflectivity zones, since Ruskin (1967) indicates that this device is only responsive to liquid droplets. On the other hand it is also noted that there is rarely an updraft of any consequence which corresponds to the high radar reflectivity zones.

It can be concluded from the relatively high readings on the JW LWC device, which only occur in the strong updrafts and not in the high radar reflectivity zones, that these updrafts contain large concentrations of liquid cloud droplets of less than 50 um diameter. It can also be concluded that the high radar reflectivity zones contain few liquid droplets less than 50 um diameter since the JW LWC gives near zero readings in these areas.

7.3 High Reflectivity Versus Turbulence

All penetrations encountered at least moderate turbulence and more frequently severe turbulence in the high radar reflectivity part of the cloud except penetration 21 June-1 (Fig. 8A).

It appears even more relevant to talk about the turbulence encountered in the main updraft areas of the storms penetrated. These areas of major updraft indicate turbulence of no greater than moderate

intensity. This is contrasted with the smooth updrafts reported at cloud base (Auer and Sand, 1966; Auer and Marwitz, 1968; and Marwitz and Berry, 1970).

This agrees well with measurements in Oklahoma reported on by Burnham and Lee (1969) where they too found the most severe turbulence associated with the highest radar reflectivities during penetrations made between 7.01 and 11.28 km MSL (23,000 and 37,000 ft). The observations do not agree with doppler radar measurements (Donaldson and Wexler, 1969) which indicate that the most severe turbulence is above the 0C isotherm and above 4.5 km (15,000 ft) in close association with strong updrafts.

Note also the severe turbulence in the updraft spike encountered during penetration 22 July-2 (Fig. 8F) just along the trailing edge of the high radar reflectivity zone. This unusual severe turbulence encounter in a strong updraft may be due to the unusual character of this updraft being behind the high reflectivity zone.

7.4 High Reflectivity Versus Hail

Normally it is expected that low reflectivity areas do not contain hail. It can be easily noted from the vertical sections that this was not always the case. Note especially 7 July-2, 7 July-4, 22 July-2 and 22 July-3 (Figs. 8D-G). During these penetrations hail was encountered in areas with relatively low reflectivities (less than 40 dBz). This can be explained by the fact that it is possible to have small hail with reflectivities less than the minimum value of 40 dBz used as the threshold for study of high reflectivity zones in this work. Using the equation $Z = \Sigma\, nD^6$ and taking D = 5 mm and n = 1 m^{-3} and converting to dBz one finds that this size and concentration yields a reflectivity of 42 dBz. Therefore, if the stones were in the pea size range with

concentrations of about 1 m^{-3} it would be possible to have hail with a reflectivity less than the 40 dBz. Auer (1972) gives a complete curve of hail size versus concentration that will produce a radar reflectivity of 40 dBz.

It is also possible that the time-space location of the radar echo and the aircraft data could differ enough in some of these cases to account for low reflectivity where significant hail was encountered. The possibility of this being the case is especially obvious on the penetration of 7 July-2 (Fig. 8D) where a slight displacement of the track or the radar echo would put the hail inside the 40 dBz contour. Penetration 22 July-3 (Fig. 8G) is obviously a case of a space-time discrepancy (as discussed in section 5.3.4) when constructing the vertical section. The size and quantity of hail encountered would be representative of the high dBz values just below the aircraft track on the vertical section.

The high radar reflectivity zones depicted in Figs. 8A-G and 9A-G have a structure which indicates their nonuniform composition. Dennis et al. (1970) postulate that these areas consist of concentrations of hail and state that these local areas of high reflectivity can be tracked down through the cloud. This type of structure can easily be seen in the vertical sections of Figs. 8A-G and especially in the vertical section of penetration 22 July-3 (Fig. 8G) which appears to contain three or four areas of locally high reflectivity at different levels in the cloud.

By referring to Table 2 it can be noted that in most cases the hail encounters consisted of quite monodisperse hailstones. The 22 July-2 and 22 July-3 (Figs. 8F and 8G) penetrations are exceptions

since a graduation in hailstone sizes was observed. During penetrations 22 July-2 (Fig. 8F) the graduation was from pea size to marble size as the penetration progressed into the high radar reflectivity zone from the front side of the cloud. The 22 July-3 penetration (Fig. 8G) experienced a pea to 1.9 cm (3/4 in) diameter hail size graduation, but this time the penetration was progressing from the rear side of the hailstorm toward the front side. Hail seems to be largest towards the center of the high radar reflectivity zones as one might expect.

It can be concluded from these penetrations that the largest hail occurred in the areas of the strong reflectivity gradients and along the edges of the strong updrafts. Hail can be found in areas where the reflectivity is less than 40 dBz.

7.5 High Reflectivity Versus Icing

It is very difficult to say much about icing relative to the high reflectivity zones since the only source of icing data is the pilot's comments made at infrequent intervals. Conclusions relative to icing can be made but are speculative due to the paucity of data and should be considered preliminary.

The airframe icing of consequence does not seem to be associated with the high JW LWC readings. High airframe icing rates do seem to be associated with the active growing parts of the cloud, i.e. the areas ahead of the high radar reflectivity zones. Obviously the high airframe icing rates are a result of supercooled drops larger than 50 um diameter striking the airframe and freezing. Severe icing is usually in the form of clear ice while light and moderate icing are usually in the form of rime ice.

Special attention should be called to penetration 7 July-4 (Fig.

8E) where 3.8 cm (1 1/2 in) of clear ice accumulated on the aircraft during the penetration. It should be noted that this was predominantly clear ice and flowed back over the top of the wings of the T-28. This was the only penetration during 1972 where such large quantities of clear ice were accumulated so rapidly.

Only penetration 21 June-2 (Fig. 8B) encountered icing of any consequence close to the high reflectivity zone. All other penetrations reported either no comment on icing or light icing in the high radar reflectivity zones. This would indicate that most of the hydrometeors in the high reflectivity zone are frozen.

7.6 High Reflectivity Versus Lightning

Lightning was only noted and recorded by the pilot when it was visually observed during a penetration so the lightning data are not complete. It can be noted from Figs. 8A-G that the lightning observations seemed to be related to the high reflectivity zones but seem to be more related to the date. Pentrations made on 7 July (Figs. 8C-E) seemed to contain the most lightning, but this was the most severe storm penetrated.

Penetration 7 July-4 (Fig. 8E) contained more lightning than any of the other penetrations with most of it occurring in the area of high reflectivity. Penetrations 7 July-1 and 7 July-2 (Figs. 8C and 8D) also contained a number of lightning observations and in both cases these were associated with the areas of high radar reflectivity. Penetration 21 June-2 (Fig. 8B) was the only other penetration where lightning was observed but it was in the area well ahead of the high radar reflectivity zone..

The storm on 7 July produced more hail than any of the other

storms penetrated. These lightning observations made in that storm tend to agree with observations made by Smith (1968) in that the more severe hailstorms are associated with occasional to frequent lightning observations.

8. SUMMARY AND CONCLUSIONS

An analysis of seven T-28 armored aircraft thunderstorm penetrations has been made using data gathered by the aircraft system and a 10 cm radar. These data have been plotted in a form suitable for analysis and combined with detailed pilot's observations of such things as hail, turbulence, icing, and lightning to form a picture of the composition of hailstorms with emphasis on the high radar reflectivity zones of thunderstorms.

It is concluded from this study that:

1. The major updrafts are not in the high reflectivity zones and in fact are not always in the weak echo region immediately ahead of the high reflectivity zones. They are often found well ahead of the high reflectivity zones in areas which appear to be new areas of development.

2. High concentrations of liquid cloud droplets are not found in the high reflectivity zones but instead are found in the updraft areas.

3. The high reflectivity zones are found to be quite turbulent with a turbulence intensity of moderate to severe. Major updraft areas are normally relatively smooth with turbulence no greater than moderate.

4. Hail is normally found along the high radar reflectivity gradients with a graduation of sizes yielding the large size in the stronger radar reflectivity zones. Hail is sometimes found outside the 40 dBz contour.

5. Little airframe icing of consequence takes place in the high radar reflectivity zones indicating that the water there is predominantly frozen. Significant airframe icing does occur in the updraft areas indicating the presence of supercooled liquid hydrometeors.

6. Based on this study little can be said about the relationship of lightning to the high radar reflectivity zones. There is an indication that hailstorms which produce significant hail also produce more lightning.

9. RECOMMENDATIONS

Penetrations of thunderstorms with this unique research tool shou be continued. The T-28 capability should be expanded to more effectiv gather significant data from the interior of thunderstorms to help man understand this phenomenon of nature.

The CPR-2 radar system has tremendous potential for gathering detailed scientific data on thunderstorms. This combination of the T-28 radar system, mesonet and other scientific aircraft available to NHRE should be used in a better, more efficient and more coordinated manner to gather the most and best scientific data possible on thunderstorms while the opportunity presents itself. Better radar data including, better real-time displays, a quick recall capability and hard copy radar data in a usable form would be extremely helpful. Operational procedures should be developed which would allow all research and seeding operations to be conducted simultaneously. The T-28 system should be used wherever possible to acquire data as part of the NHRE project.

The T-28 system should be expanded to measure the diffusion and the effectiveness of seeding materials. The T-28 should be used to determine the airflow structure inside thunderstorms. Equipment should be acquired or developed so the T-28 can determine the entire hydrometeo spectra in both size and number concentration. All these measurements depend on the acquisition (and in some cases the development) of specia instruments for the measurement of these various properties of thunderstorms.

ACKNOWLEDGMENTS

This research was supported under Prime Contract No. NSF-C460, Subcontract No. NCAR 182-71 as part of the research on the National Hail Research Experiment sponsored by the Weather Modification Program, RANN, National Science Foundation.

Acknowledgment is made to the National Center for Atmospheric Research, which is sponsored by the National Science Foundation, for computer time used in this research.

Thanks are gratefully extended to Mr. Jerry Halvorson and Mr. Garth Peterson of the IAS staff and Mr. Carl Mohr and Mrs. Betty Stobie of the NCAR staff for their programming efforts. Mr. Dean House of the Desert Research Institute is thanked for the radar tracks provided. Mr. Chuck Jasper and Mr. Leonard Block of the IAS staff and Mr. Dennis King of the NCAR staff are thanked for their assistance in keeping the aircraft and instrumentation in a very fine operating condition during the 1972 field season.

Mr. Dennis Musil of the IAS staff who acted as both radar meteorologist at Grover during all of the 1972 thunderstorm penetrations and also as my major professor is very gratefully thanked for his very able assistance in all phases of this work.

Dr. R. A. Schleusener must be thanked for his overall supervision of the entire T-28 project. He has maintained the faith and determination over the years to make the project work. He has given me many ideas and helpful suggestions when they were most needed.

Lastly, I thank my wife Bobbie for her patience while preparing this work and for her typing efforts on the manuscript.

REFERENCES

Aerographer's Mate 1 and C, 1969: Bureau of Naval Personnel, Rate Training Manual. NAVPERS 10362-A. Stock Ordering No. 0500-112-005(819, p. 380.

Appleman, H. S., 1971: Lightning hazard to aircraft. HQ Air Weather Service, Technical Report 179 (Rev), 10 pp.

Auer, A. H., Jr., and W. Sand, 1966: Updraft measurements beneath the base of cumulus and cumulonimbus clouds. J. Appl. Meteor., 5, 461-466.

_____, and J. W. Marwitz, 1968: Estimates of air and moisture flux into hailstorms on the High Plains. J. Appl. Meteor., 7, 196-198.

_____, 1972: Distribution of graupel and hail with size. Mon. Wea. Rev., 100, No. 5, 325-328.

Booker, D. R., L. W. Cooper, and H. E. Hart, 1967: Updraft and air flux studies utilizing instrumented aircraft and superpressure balloon-transponder systems. Final Report, Contract E 22-79-67 (N), 35 pp.

Browning, K. A., 1964: Airflow and precipitation trajectories within severe local storms which travel to the right of winds. J. Atmos. Sci., 21, 634-639.

Burnham, J., and J. T. Lee, 1969: Thunderstorm turbulence and its relation to weather radar echoes. Journal of Aircraft, 6, No. 5, 438-445.

Bushnell, R. H., 1973: Dropsonde measurements of vertical winds in th Colorado thunderstorm of 22 July 1972. J. Appl. Meteor., 12, 1371-1374.

Byers, H. R., and R. R. Braham, 1949: The Thunderstorm. U. S. Government Printing Office, Washington, D. C., 298 pp.

Chisholm, A. J., 1968: Observations by 10-cm radar of an Alberta hailstorm in a sheared environment. Proc. Thirteenth Radar Meteor. Conf., 82-87.

_____, and M. English, 1973: Alberta hailstorms. Meteor. Monogr., 14, No. 36, 98 pp.

Dennis, A. S., C. A. Schock, and A. Koscielski, 1970: Characteristics of hailstorms of western South Dakota. J. Appl. Meteor., 9, 127-135.

_____, P. L. Smith, Jr., E. I. Boyd, and D. J. Musil, 1971: Radar observations of hail in western Nebraska. Report 71-1, Institute of Atmospheric Sciences, South Dakota School of Mines and Technology, Rapid City, South Dakota, 42 pp.

Donaldson, R. J., Jr., and R. Wexler, 1969: Flight hazards in thunderstorms determined by doppler velocity variance. J. Appl. Meteor., 8, 128-133.

Eccles, P. J., 1973: Dual-wavelength observations of a hailstorm. Preprints, Eighth Conference of Severe Local Storms, Denver, Colorado, Amer. Meteor. Soc., 52-56.

Foote, G. B., and J. C. Fankhauser, 1973: Airflow and moisture budget beneath a northeast Colorado hailstorm. J. Appl. Meteor., 12, 1330-1353.

Hart, H. E., and L. W. Cooper, 1968: Thunderstorm airflow studies using radar transponders and superpressure balloons. Proc. Thirteenth Radar Meteorology Conf., Boston, Amer. Meteor. Soc., 196-201.

Hirsch, J. H., 1971: Computer modeling of cumulus clouds during Project Cloud Catcher. Report 71-7, Institute of Atmospheric Sciences, South Dakota School of Mines and Technology, Rapid City, South Dakota, 61 pp.

Johnson, G. N., 1974: Distinctive features of the T-28 data system. Accepted for publication in Atmospheric Technology.

Kyle, T. G., 1974: Thunderstorm turbulence. Unpublished personal communication.

_____, and W. R. Sand, 1973: Water content in convective storm clouds. Science, 180, 1274-1276.

MacCready, P. B., Jr., 1964: Standardization of gustiness values from aircraft. J. Appl. Meteor., 3, 439-449.

Marwitz, J. D., and E. X. Berry, 1971: The airflow within the weak echo region of an Alberta hailstorm. J. Appl. Meteor., 10, 487-492.

_____, 1972a: The structure and motion of severe hailstorms. Part I: Supercell storms. J. Appl. Meteor., 11, 166-179.

_____, 1972b: The structure and motion of severe hailstorms. Part II: Multicell storms. J. Appl. Meteor., 10, 180-188.

_____, 1972c: The structure and motion of severe hailstorms. Part III: Severely sheared storms. J. Appl. Meteor., 10, 189-201.

_____, 1973: Trajectories within the weak echo regions of hailstorms. J. Appl. Meteor., 12, 1174-1182.

Miller, E., 1968: Synopsis of a thunderstorm research program (Roughrider) for 1966-1967. Air Force Systems Command, Technical Report ASD-TR-68-29, 52 pp.

Musil, D. J., W. R. Sand, and R. A. Schleusener, 1973: Analysis of data from T-28 penetrating aircraft. J. Appl. Meteor., 12, 1364-1370.

Newton, C. W., 1963: Dynamics of severe convective storms. Meteor. Monogr., 5, No. 27, 33-58.

Phillips, B. B., 1973: Precipitation characteristics of a sheared, moderate intensity, supercell-type Colorado thunderstorm. J. Appl. Meteor., 12, 1354-1363.

Ruskin, R. E., 1967: Measurements of water-ice budget changes at -5C in AgI-seeded tropical cumulus. J. Appl. Meteor., 6, 72-81.

Sand, W. R., R. A. Schleusener, and J. H. Hirsch, 1972a: Final report on T-28 armored aircraft during the period 1 May 1970 - 1 May 1971. Report 72-4, Institute of Atmospheric Sciences, South Dakota School of Mines and Technology, Rapid City, South Dakota, 33 pp.

_____, _____, and D. J. Musil, 1972b: Final report of the T-28 armored aircraft during the period 1 May 1971 - 1 May 1972. Report 72-17, Institute of Atmospheric Sciences, South Dakota School of Mines and Technology, Rapid City, South Dakota, 55 pp.

_____, _____, _____, 1973: Final report of T-28 armored aircraft during the period 1 May 1972 - 1 May 1973. Report 73-11, Institute of Atmospheric Sciences, South Dakota School of Mines and Technology, Rapid City, South Dakota, 23 pp.

_____, _____, _____, 1973: Observed updrafts and hail inside a thunderstorm. J. Wea. Mod., 5, No. 1, 24-29.

Sinclair, P. C., 1969: Vertical motion and temperature structure of severe convective storms. Preprints Sixth Conference on Severe Local Storms, Chicago, Illinois, Amer. Meteor. Soc., 346-351.

Smith, M. D., 1968: A correlation study of hail and lightning. Proc. International Conf. on Cloud Physics, Toronto, Canada, 460-463.

Sulakvelidze, G. K., H. Sh. Biblashvili, and V. F. Lapcheva, 1967: Formation of precipitation and modification of hail processes. Translated by Israel Program for Scientific Translations, Jerusalem, 208 pp.

Summers, P. W., and L. Wojtiw, 1971: The economic impact of hail damage in Alberta, Canada and its dependence on various hailfall parameters. Preprints Seventh Conference on Severe Local Storms, Kansas City, Mo., Amer. Meteor. Soc., 158-163.

Swinbank, W. C., 1970: Plan for the National Hail Research Experiment (NHRE). NCAR publication, 21 pp.

Williamson, R. E., 1969: Aircraft probing of hailstorms. Final report by Meteorology Research Incorporated to Institute of Atmospheric Sciences, South Dakota School of Mines and Technology, Rapid City, South Dakota. (MRI 69 FR-841), 24 pp.

APPENDIX A

CPR-2 RADAR PARAMETERS*

S-band Antenna:

Aperture area: $56.5 m^2$

Horizontal polarization

Beamwidth: 1.0°

Max angular velocity: 12° sec-1

Scan: Automatic raster scan of storm with controllable limits in both azimuth and elevation.

S-band Transmitter:

Generic type: FPS/18

Wavelength 10.4 cm

Frequency: 2803 MHz

Peak power: 250 kW

Pulse duration: 1.2 microsec

PRF: pulse jittered, 1071 and 1250 pps, to eliminate range ambiguity of 2nd trip echoes.

S-band Receiver:

Minimum detectable signal: -108dBm

* Taken from: Eccles, P. J., 1973: Dual-wavelength observations of a hailstorm. Preprints, 8th Conf. of Severe Local Storms, Denver, Colo., 52-56.

VITA

Wayne Russell Sand was born in Conrad, Montana on 2 March 1941. He graduated from Valier High School at Valier, Montana on 25 May 1959. He graduated from Montana State University at Bozeman, Montana on 10 June 1963. He attended graduate school at Montana State University and Colorado State University prior to entering the U. S. Navy on 26 March 1966. On 10 May 1974 he received a Master of Science degree in Meteorology from the South Dakota School of Mines and Technology, Rapid City, South Dakota.

During the summers of 1961 and 1962 he worked on a commercial weather modification project in Montana. While at Colorado State University he worked in the field of weather modification research from May 1964 until March 1966.

While in the U. S. Navy from March 1966 to March 1971 he attained the rank of Lieutenant and was designated a Naval Aviator on 5 Oct. 1967. He was chosen the outstanding Student Naval Aviator of the Year 1967. He went on to fly the Grumman A-6 aircraft in Southeast Asia and in the Mediterranean from the decks of aircraft carriers. He served in a test and evaluation squadron where he was a project officer in charge of weapons evaluation.

Since 1 April 1971 he has been a professional employee of the South Dakota School of Mines and Technology.